UNIVERSIDADE DE LISBOA

FACULDADE DE CIÊNCIAS

DEPARTAMENTO DE FÍSICA

Image-guided drug delivery using Fe-deferoxamine loaded temperature-sensitive liposomes

ADRIANA MARTINS FERNANDES

Dissertação

Orientadores
Prof. Dr. Holger Grüll
Prof. Dr. Nuno Matela

Mestrado Integrado em Engenharia Biomédica e Biofísica
Perfil em Radiações em Diagnóstico e Terapia
-2015-

Resumo

A predominância de cancro está a aumentar nos países ocidentais uma vez que a população se encontra cada vez mais envelhecida. A quimioterapia é uma das abordagens mais utilizadas, no entanto, existe a necessidade de aumentar a absorção dos fármacos nos tumores. Um modo com vista a reduzir os efeitos secundários negativos para o paciente é a entrega de fármacos, induzida pela temperatura. Este conceito está relacionado com lipossomas sensíveis à temperatura que encapsulam fármacos que irão atuar como agentes de quimioterapia. Estes fármacos são libertados mediante o aquecimento a temperaturas em torno dos 42 ºC. A esta temperatura a bicamada lipídica experimenta uma transição de fase, o que por sua vez intermedeia uma rápida entrega de fármaco. Uma distribuição localizada do fármaco é conseguida aquecendo a área central do tumor.

O conceito acima apresentado foi estendido à entrega localizada de fármacos guiada por imagem, ao encapsular adicionalmente um agente de contraste no lipossoma. Ao encapsular tanto o fármaco, neste caso a doxorubicina, como o agente de contraste, para ressonância magnética à base de *gadolinium,* é possível quantificar a entrega de fármaco induzida pela temperatura. Uma vez libertado o agente de contraste do lipossoma dá-se uma variação no contraste nas imagens de ressonância magnética, o que possibilita quantificar a dose de fármaco libertado no tumor.

A utilização de lipossomas sensíveis à temperatura, que encapsulem tanto doxorubicina como *gadolinium* (Gd), potenciam a avaliação da eficácia da entrega do fármaco no tumor. A taxa de relaxação longitudinal traduz-se no inverso do tempo de relaxação T_1. Os agentes de contraste permitem a redução dos tempos de relaxação característicos da ressonância magnética, melhorando o contraste das imagens, o que permite uma melhor diferenciação das estruturas presentes. Foi demonstrado anteriormente que existe uma boa correlação entre a absorção de fármaco, a concentração do agente de contraste e a taxa de relaxação longitudinal do agente de contraste (R_1) no tumor.

No entanto, a utilização de lipossomas paramagnéticos, que encapsulem agentes de contraste em ressonância magnética à base de Gd pode conduzir à toxicidade induzida pelo Gd. Isto acontece pois os lipossomas são preferencialmente depurados pelo fígado e baço, o que leva à concentração elevada de Gd^{3+} nestes órgãos. Em pacientes que sofram de insuficiência renal grave, sabe-se que a retenção prolongada deste agente de contraste à base de Gd pode conduzir a fibrose sistémica nefrogénica. Uma vez que ao encapsular Gd em lipossomas a sua depuração acontece essencialmente no baço e fígado, em oposição à depuração renal (para o Gd quando se encontra na forma livre), o agente de contraste ficará retido mais tempo no organismo o que levanta questões relativamente à segurança deste conceito.

Dado este problema, existia a necessidade de encontrar uma alternativa viável para o agente de contraste, Gd, comercialmente conhecido como ProHance®. Um estudo realizado anteriormente no grupo de investigação passou por substituir o Gd, [Gd (HPDO3A) (H_2O)], por um agente de contraste à

base de ferro, Fe^{3+}-deferoxamine (Fe^{3+}-DFO), pois o ferro tem uma via metabólica estabelecida. Infelizmente, mediante o aquecimento dos lipossomas, localmente, foi observada uma libertação gradual do agente de contraste, Fe^{3+}-DFO, em vez de uma libertação rápida e completa a uma temperatura específica, a temperatura de transição (T_m), como verificado quando se utilizou Gd como agente de contraste. A causa deste comportamento pode dever-se à hidrofobia do agente de contraste Fe-DFO, permitindo que o mesmo atravesse a bicamada ou mesmo uma associação do agente de contraste com a bicamada. Adicionalmente, o encapsulamento tanto do agente de contraste Fe-DFO como do fármaco doxorubicina aboliu o tempo de relaxação T_1, possivelmente devido à formação de óxidos de ferro ou agregações de doxorubicina com o ferro. Outro ponto negativo do encapsulamento de Fe-DFO em lipossomas sensíveis à temperatura prende-se com o baixo valor de pH de solução tampão intralipossomal requerido, de modo a possibilitar um encapsulamento estável do complexo dentro do lipossoma. Isto pode levar à hidrólise da bicama limitando assim o tempo de vida do produto resultante.

O objetivo deste projeto passou por usar um agente de contraste derivado de Fe^{3+}-deferoxamine, mas mais hidrófilo, deferoxamine-N-succimidyl Fe(III), DFO-N-Suc-Fe (III), assim como uma formulação lipossomal diferente, de modo a resolver o problema observado. Este agente de contraste poderia ser utilizado para monitorizar a libertação de doxorubicina de lipossomas sensíveis a temperatura (TSLs). A aplicação final seria a quantificação da dose de fármaco utilizada na quimioterapia ao utilizar TSLs juntamente com ultrassons focados de alta intensidade guiados por ressonância magnética.

Em estudos anteriores já enunciados, ao encapsular tanto a doxorubicina como o Fe^{3+}-DFO em lipossomas a relaxividade foi perdida. Deste modo, em primeiro lugar, ao invés de encapsular os dois compostos num mesmo lipossoma, lipossomas com doxorubicina e lipossomas com agente de contraste serão co injetados. Em segundo lugar, ao variar a formulação lipídica que constitui os lipossomas, tentou-se ajustar a estabilidade e as propriedades de libertação dos lipossomas ao encapsular o agente de contraste. Por fim, o agente de contraste à base de ferro foi adaptado de modo a conseguir um encapsulamento mais estável.

As medições da taxa de relaxação longitudinal, R_1, em função da temperatura indicaram que a libertação do agente de contraste, DFO-N-Suc-Fe (III), de lipossomas tradicionais sensíveis a temperaturas aconteceu entre 41 ºC e 42 ºC, em contraste com a temperatura a que o agente de contraste Fe-DFO foi libertado do mesmo tipo de lipossomas (entre 42 ºC e 45 ºC). Além disto a libertação do agente de contraste, DFO-N-Suc-Fe (III), foi rápida, ao contrário da libertação do agente de contraste Fe-DFO, que se deu gradualmente. Medições a temperaturas constantes revelaram 100 % de libertação do agente de contraste, DFO-N-Suc-Fe (III), passados 15 minutos e cerca de 80 % de libertação passados apenas 5 minutos. Este tempo de libertação pode ser melhorado ajustando a formulação lipídica. Estes lipossomas revelaram-se muito estáveis à temperatura corporal o que se revelou uma melhoria considerável quando comparados com lipossomas que encapsulavam Fe-DFO.

Lipossomas sensíveis à temperatura que encapsulavam o complexo DFO-N-suc-Fe (III) foram adicionalmente diluídos em solução tampão para testes de caraterização *in vitro.* Os tempos de relaxação

longitudinal e transversal T_1 e T_2, respetivamente, foram medidos num scanner clínico de ressonância magnética de 3 T, antes e depois de aquecer os lipossomas durante 30 minutos, a 45 ºC. Antes de aquecer os lipossomas, diferentes concentrações do complexo DFO-N-suc-Fe (III) assumiram um valor de T_1 menor quando comparado com o valor da mesma amostra após o aquecimento. Esta experiência veio mostrar o potencial da imagem de ressonância magnética, quando combinada com lipossomas sensíveis à temperatura.

O objetivo desta investigação passou por melhorar a libertação lipossomal do agente de contraste, assim como a estabilidade da formulação lipossomal. Ambas as melhorias, na libertação e estabilidade, foram obtidas através da adaptação do complexo Fe-DFO utilizado inicialmente, o que permitiu um pH intralipossómico mais elevado, minimizando assim o risco de hidrólise. A associação de Fe-DFO com a doxorubicina foi evitada, optando por uma co-injeção em vez de um co-encapsulamento.

Os passos seguintes incluem pequenas adaptações à formulação lipídica, numa tentativa de encapsular mais agente de contraste. Quando a formulação estiver completamente aperfeiçoada deverá também ser estudado o mesmo sistema para a doxorubicina. O último passo será a injeção *in vivo* de modo a quantificar a dose de fármaco administrada no tumor por meio de lipossomas sensíveis à temperatura, utlizado um agente de contraste à base de ferro.

Verificando-se eficácia *in vivo,* esta classe de agentes de contraste criará oportunidades na libertação monitorizada de fármaco com recurso a ressonância magnética, em resposta a hipertermia local, evitando os inconvenientes de agentes de contraste à base de Gd.

Palavras-chave: lipossomas sensíveis a temperatura, administração localizada de fármaco, ultrassom focal de alta intensidade guiado por ressonância magnética, agentes de contraste, ferro

Abstract

The predominance of cancer is rising in western countries since a demographic change in the direction of an aging society is happening. Chemotherapy is one of the standard treatments but there is a need to increase the uptake of drug in tumors. One approach to reduce negative side effects to the patient is temperature-induced drug delivery. This concept regards temperature-sensitive liposomes encapsulating a drug that will act as a chemotherapy agent. This drug will be released upon heating to a mild hyperthermia (around 42 ºC). At this temperature the lipid bilayer experiences a phase transition that will intermediate a fast drug delivery. Local drug delivery can be achieved by focal heating of the tumor area.

The concept presented above was extended to image-guided drug delivery so a contrast agent is encapsulated in the liposome as well. By encapsulating both the drug doxorubicin and a gadolinium-based magnetic resonance (MR) agent it is possible to quantify the temperature-induced drug delivery. Upon contrast agent release from the liposome, a contrast change on the MR images is created which will enable the quantification of released drug in the tumor.

However, the use of paramagnetic liposomes employing gadolinium (Gd)-based MRI contrast agent might lead to Gd-induced toxicity since the liposomes are preferentially cleared by the liver and spleen, which leads to a high Gd^{3+} concentration in these organs. From patients suffering from severe renal impairment, it is known that prolonged retention of Gd-based contrast agent may lead to nephrogenic systemic fibrosis (NSF). As the liposomal encapsulation of [Gd(HPDO3A)(H_2O)] will lead to preferential liver and spleen clearance, as opposed to renal clearance for the free contrast agent, the contrast agent will have a longer retention time in the body, raising questions about the safety of the concept. There was a need of finding an alternative for [Gd(HPDO3A)(H_2O)], (ProHance®), a clinically approved contrast agent, so in a previous in-house study [Gd(HPDO3A) (H_2O)] was replaced by Fe^{3+}-deferoxamine (Fe^{3+}-DFO) since iron has an established metabolic pathway. Unfortunately, a gradual release of Fe^{3+}-DFO from the liposomes was observed upon heating, instead of a rapid and complete release at the melting phase transition temperature (T_m).

The aim of this research was to improve the liposomal release of the CA as well as the stability of the liposomal formulation. Both improvements in release and stability were achieved by adapting the Fe^{3+}-DFO complex used previously, to deferoxamine-N-succimidyl Fe(III), DFO-N-Suc-Fe (III), which allowed a higher intraliposomal pH, thereby minimizing the risk of hydrolysis. The association of Fe-DFO with doxorubicin was avoided by opting for a co-injection instead of co-encapsulation.

This contrast agent can be used to monitor drug release from doxorubicin-loaded temperature-sensitive liposomes (TSLs). The end application would be the drug-dose painting for TSLs containing chemotherapy delivered by MR-guided HIFU (High Intensity Focused Ultrasound).

Key words: temperature-sensitive liposomes, local drug-delivery, magnetic resonance-guided high intensity focused ultrasound, contrast agents, iron

Abbreviations

Abbreviation	***Description***
CA	Contrast agent
Cryo-TEM	Cryogenic transmission electron microscopy
DDS	Drug delivery systems
DFO	Deferoxamine
DLS	Dynamic light scattering
Dox	Doxorubicin
DPPC	1.2-dipalmitoyl-*sn*-glycero-3-phosphatidylcholine
DPPE-PEG2000	1.2-dipalmitoyl-sn-glycero-3-phosphoethanolamine-N-[methoxy(polyethylene glycol)2000]
DPPGOG	1.2-dipalmitoyl-sn-glycero-3-phosphoglyceroglycerol
DSC	Differential scanning calorimetry
DSPC	Distearoly-*sn*-glycero-3-phosphatidylcholine
EPR	Enhanced permeability and retention
FBS	Fetal bovine serum
Fe^{3+}-DFO	Fe^{3+}-deferoxamine
FID	Free induction decay
Gd	Gadolinium
Gd(III)HPDO3A	Gadoteridol
GE	Gradient echo
HBS	HEPES-buffered saline solution
HIFU	High Intensity Focused Ultrasound
HSPC	L-*α*-Phosphatidylcholine
HT	Hyperthermia
ICP-IOS	Inductively coupled plasma optical-emission spectroscopy
IR	Inversion recovery
iTLSs	Imageable TSLs
LL	Look-Locker
LMVs	Large multilamellar vesicles
LTSL	Low temperature sensitive liposomes
LUVs	Large unilamellar vesicles
MPPC	1-palmitoyl-*sn*-glycero-3-phospho-choline
MR	Magnetic resonance
MRI	Magnetic resonance imaging
NSF	Nephrogenic systemic fibrosis
MSPC	1-stearoyl-sn-glycero-3-phospho-choline
MW	Molecular weight
NMR	Nuclear magnetic resonance
NP	Nanoparticle
NTSLs	Non-temperature-sensitive liposomes
PBS	Phosphate buffered saline
PDI	Polydispersity index
PEG	Polyethylene glycol
R_1	Longitudinal relaxation rate
r_1	Longitudinal relaxivity

R_2	Transverse relaxation rate
r_2	Transverse relaxivity
RD	Recovery delay/recycle delay
RES	Reticuloendothelial system
RF	Radio frequency
ROI	Region of interest
RT	Room temperature
SE	Spin echo
T_1	Longitudinal relaxation time
T_2	Transverse relaxation time
T_m	Melting phase transition temperature
TSLs	Temperature-sensitive liposomes
TTSLs	Traditional temperature-sensitive liposomes

Contents

1. State of the Art

1.1. Cancer Treatment

The predominance of cancer is rising in western countries since a demographic change in the direction of an aging society is happening. In order to increase treatment efficiency earlier diagnosis and new treatment options are essential. Most common treatments range from invasive surgery to non-invasive radiotherapy, chemotherapy or a combination depending on the cancer and its stage [1]. In all the cases, the main goal is to eliminate all cancerous tissue in the body while minimizing harm to healthy tissues.

The surgical removal of a tumor is the first line treatment for localized tumors, however in some cases it is not possible due to lesions invading into surrounding vital structures or when tumors are impossible to reach by conventional surgery. In radiotherapy high-energy radiation is used in order to destroy cancer cells. This treatment is usually associated with a substantial burden to the patient and it can increase the risk for development of other cancers. Chemotherapy is an option for cancers that are difficult to remove surgically or that have metastasized to the rest of the body. When chemotherapy drugs are administered they circulate freely in the blood stream and attack fast dividing cells. In this fashion drugs are effective against cancer cells. However, they will also attack normal healthy cells. Side effects of chemotherapy include anemia[i], neutropedia[ii], bleeding and an increased risk of opportunistic infections. The side-effects are sometimes treatment-limiting which limits the tolerable chemotherapy dose to a level below the required dose for optimum treatment. For some cancers a more localized chemotherapy treatment would allow an increase in the dose that is delivered to the tumor without increasing the dose that is delivered to the rest of the body. This could expand the effectiveness of the treatment. Moreover, the blood supply to tumors is notoriously inhomogeneous. This implies that some parts of the tumor can be well perfused with blood and others poorly perfused. Chemotherapy drugs are not taken up evenly so poorly perfused areas will receive a sub-optimal dose. Thus, a way to quantify the drug delivery process *in vivo* while the therapy is ongoing would be an indispensable tool for a physician as it allows to judge whether a treatment is successful and suited for the particular patient or whether an alternative treatment should be considered.

Even though significant progress has been made in cancer therapy, many cancers are still not curable with these treatments. There is need to improve treatment possibilities, to assess treatment efficacy and to reduce the burden to the patient. Increasing local chemotherapy uptake may improve the effectiveness

[i] Reduced red blood cell count
[ii] Reduced white blood cell count

of the therapy and limit the side effects. In this thesis a temperature-sensitive drug delivery system was studied in order to develop a way to monitor the efficacy of this kind of treatment in tumors.

1.2. Liposomal Drug Delivery

In classical chemotherapy cytotoxic drugs are administered systemically and they spread throughout the body. One of the main problems presented by this kind of approach is that healthy tissues are also intoxicated, which will limit the tolerable drug dose and therefore also the achievable drug concentration in the tumor.

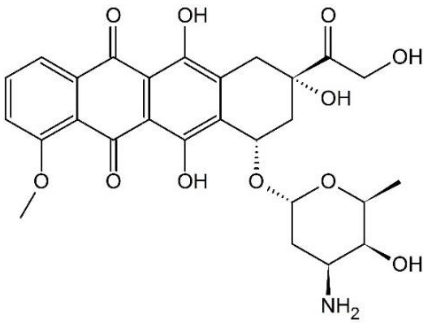

Figure 1. *Chemical structure of doxorubicin.*

Doxorubicin is a commonly used chemotherapeutic drug, Figure 1, that has a substantial antitumor activity against numerous human malignancies which includes leukemia and breast cancer [2,3]. The disadvantage of using doxorubicin in the clinic is its cumulative and irreversible cardiotoxicity, myelosuppression[iii], and the occurrence of drug resistance [4].

Nanomedicine is the application of nanotechnology to healthcare and it is a quickly evolving field, showing great promise to improve current treatment regimes. In order to reduce systemic toxicity, the drug can be placed inside new nanomolecules as liposomes[iv]. Liposomes are microscopic artificial spherical structures that are formed by one or several concentric lipid bilayers with an inner aqueous compartment. This class of nanovesicles have been widely explored and studied specifically in the area of biomedicine for early diagnosis and treatment of diseases. In pioneering studies in 1961, Bangham et al. revealed the self-assembly of phospholipids into liposomes wherein a single continuous bilayer of phospholipids splits the external aqueous medium from the liposomal aqueous lumen.

[iii] Decrease in the production of cells that are responsible for providing immunity (leukocytes) and carrying oxygen (erythrocytes)

[iv] Artificial spherical vesicles (lipidic nanoparticles) that are formed by one or several concentric lipid bilayers with an inner aqueous compartment

Lately, numerous liposomal drug formulations have been clinically approved in oncology [5] and they are characterized by passive uptake in the tumor. Though plenty of nanostructures have been investigated, liposomes are one of the most promising systems thanks to their composition in low toxicity lipids and their biocompatibility. Using this approach many of the pharmacological properties of the conventional free drugs can be altered by using drug delivery systems, DDS [6], which embrace specific carriers, composed of lipids or polymers and their associated therapeutics [7,8]. Liposomal doxorubicin formulations that are sterically-stabilized such as Caelyx®/Doxil® showed reduced cardiac toxicity comparing to unencapsulated doxorubicin [9]. Long-circulating liposomes such as these accumulate in tumor tissue thanks to the extravasation through leaky vasculature of tumors in combination with their poorly operating lymphatic system exploiting the enhanced permeability and retention (EPR) effect [10].

Preclinical studies with liposomal doxorubicin showed 3 to 15 fold greater peak doxorubicin levels in tumors and an enhanced of antitumor activity when compared to free doxorubicin [11].

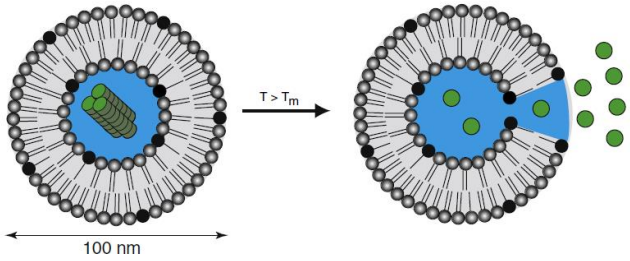

Figure 2. *Schematic representation of heat-triggered chemotherapeutic drug, dox (doxorubicin), release from a temperature-sensitive liposome. Figure from* [12].

1.2.1. Temperature-Sensitive Liposomes

Temperature-sensitive liposomes (TSLs) have the ability to release their contents near their phase transition temperature (T_m) when the lipid membrane experiences a transition from a gel to a liquid-crystalline phase. Liposomal membranes in the gel phase (i.e. solid-like) are less permeable to water and drugs compared to the liquid-crystalline phase [13].

Yatvin and Weinstein et al. [13,14] introduced the concept of temperature induced drug delivery with temperature-sensitive liposomes four decades ago by suggesting local hyperthermia[v] in order to stimulate selective delivery of liposomes which contain encapsulated drugs to target areas [13,14]. Right after the

[v] Local hyperthermia is achieved by heating a region of the body few degrees above its normal temperature [13]; The combination of local hyperthermia with temperature sensitive liposomes will lead to localized triggered drug-delivery from responsive liposomal formulations which will increase the drug concentration and its bioavailability in the tumor

intravenous injection of TSLs, the release of the content form the liposomes could occur during the passage of the liposomes through the heated tumor, as can be seen in Figure 3. This concept is currently under clinical investigation. For hepatocellular carcinoma, for example, surgical resection is inadequate or not feasible so the application of TSLs during radiofrequency ablation (RFA) would potentially address this limitation [15].

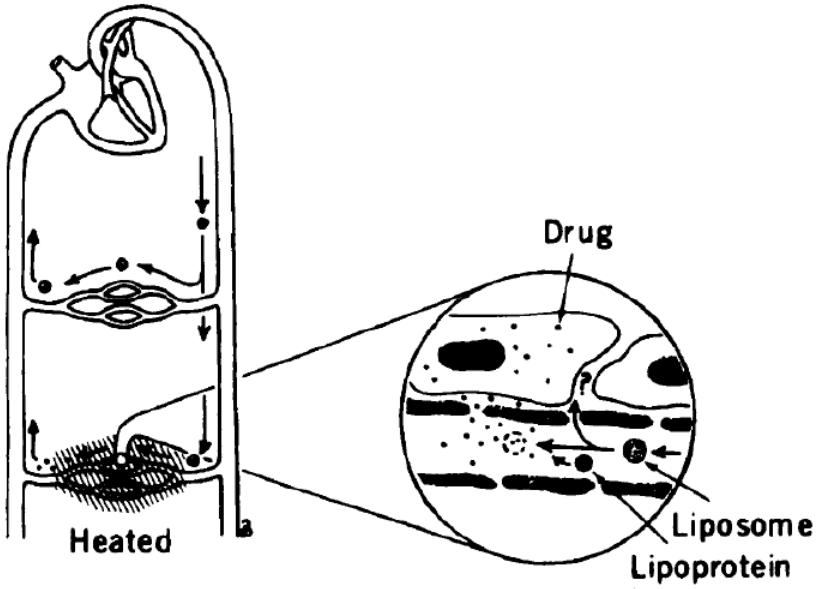

Figure 3. *Schematic representation of local drug delivery using temperature-sensitive liposomes. When liposomes enter the small vessels of the region that was heated the rate wherewith they release their content depends on the temperature and on the temperature change rate. Figure from* [13]***.***

The liposomes used by Yatvin, Weinstein and their coworkers, were prepared from two lipid components: DPPC (1.2-dipalmitoyl-*sn*-glycero-3-phosphatidylcholine) and DSPC (Distearoly-*sn*-glycero-3-phosphatidylcholine), Figure 4. DPPC was responsible for temperature sensitivity since its phase transition temperature, T_m, has a value around 41.5 ºC. On the other hand DSPC, with a T_m of near 54.9 ºC [16], was used to improve its stability at 37 ºC and to fine tune the transition temperature of the liposomal membrane. Using this formulation in a 3:1 (DPPC:DSPC) ratio the release temperature was between 42.5 ºC and 44.5 ºC. This formulation was used for temperature-induced neomycin[vi] and methotrexate[vii] delivery but it was still not optimal due to the poor blood circulation times, slow release kinetics and a lack of quantitative drug release at the melting phase transition temperature [17].

[vi] Aminoglycoside antibiotic
[vii] Synthetic compound that interferes with cell growth. Is used to treat leukemia and other forms of cancer

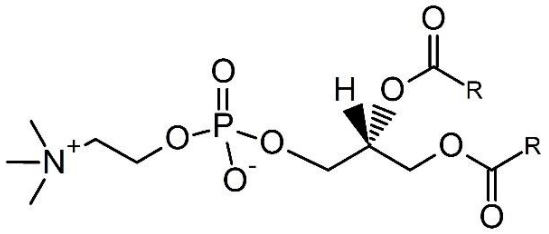

Figure 4. *Chemical structure of phospholipids used for preparation of TSLs. Phospholipid DPPC 1.2-dihexadecanoyl-sn-glycero-3-phosphocholine, (R=$C_{15}H_{31}$), and the phospholipid DSPC 1.2-dioctadecanoyl-sn-glycero-3-phosphocholine, (R=$C_{17}H_{35}$).*

In vivo studies using conventional liposomes demonstrated that interactions with serum proteins such as immunoglobulins and fibronectin, cause instability of the lipid bilayer and as a consequence, liposomes are removed from the circulation [18]. In order to improve the lipid bilayer stability cholesterol can be incorporated, which will be responsible for an increased packing of the phospholipids.

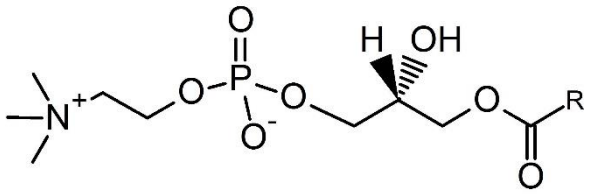

Figure 5. *Chemical structure of MPPC, 1-palmitoyl-sn-glycero-3-phospho-choline (R=$C_{15}H_{31}$), and MSPC, 1-stearoyl-sn-glycero-3-phospho-choline (R=C17H35).*

Different strategies have been developed preventing fast clearance by the RES (reticuloendothelial system). Advances in liposome research have led to the development of liposomes constructed with polyethylene glycol (PEG), also known as “stealth liposomes”, that display prolonged circulation times in the blood. PEG is added to improve stability and decrease interactions with the immune system, leading to increased blood circulation times. The flexible PEG chains occupy the space adjacent to the liposome surface. This will inhibit access and binding of the blood plasma proteins to the liposomal membrane. Their half-live times ranges from 24 to 48 hours [19]. These sterically-stabilized liposomes accumulate in tumor as a result of extravasation through the highly permeable vasculature of tumors in combination with the poorly operating lymphatic system [20]. Long circulating liposomes that encapsulated doxorubicin (e.g. Doxil®) have already been clinically approved for Kaposi sarcoma, metastatic breast cancer, ovarian cancer and several other indications [21].

Needham et.al [22] explored the use of *lyso*-PC-based temperature-sensitive liposomes (LTSLs, lysolipid-based temperature-sensitive liposomes) into the liposomal membrane such as MPPC (1-palmitoyl-sn-glycero-3-phospho-choline) or MSPC (1-stearoyl-*sn*-glycero-3-phospho-choline) for localized doxorubicin delivery combined with mild hyperthermia (between 41 ºC and 42 ºC), Figure 5. Preclinical experiments

showed more efficacy in temperature-induced drug delivery with LTSLs than with TTSLs[viii] (Traditional temperature-sensitive liposomes) since LTSLs displayed faster release of the encapsulated content [22]. Additionally, in contrast with pure DPPC/DSPC-based TSLs, when *lyso*-PC are added there is a quantitative doxorubicin release within few seconds in response to mild hyperthermia [17]. This fast release, at T_m, of the aqueous solutes is probably due to the formation of transient pores and instabilities along grain boundaries that exist in the liposomal leaflet [23]. One possible disadvantage of the *LTSLs* is their considerable high doxorubicin leakage at body temperature [24].

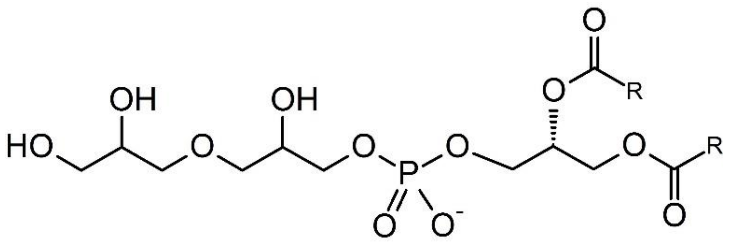

Figure 6. *Phospholipid $DPPGG_2$ (or DPPGOG) 1.2-dipalmitoyl-sn-glycero-3-phosphoglyceroglycerol.*

A novel class of temperature-sensitive liposomes based in 1.2-dipalmitoyl-sn-glycero-3-phosphoglyceroglycerol (DPPGOG), Figure 6, has been developed by Lindner at al. in 2004 [25]. These temperature-sensitive liposomes composed by DPPC/DSPC/DPPGOG (with no PEG) showed improved serum stability at 37 ºC when compared with LTSLs. Liposomes based in DPPGOG displayed a prolonged circulation time in the blood. This will lead to higher levels of dox concentration in plasma when compared with other TSL formulations [26,27].

Properties such as drug release kinetics and the blood circulation time of TSLs can be tuned by the chemical composition of the lipid bilayer. For temperature-induced drug delivery, the TSL formulation should be optimized in order to warrant a high plasma concentration of the drug over the time span of hyperthermia [12,28]. It is also important to tune TSLs to achieve fast release at the tumor site.

Currently, ThermoDox® (Celsion), the lysolipid-containing formulation is ongoing clinical trials and a phase I clinical trial for patients with primary and metastatic tumor of the liver is now completed. For this study patients were treated with RF ablation in combination with ThermoDox® which was safe and more efficient than with RF ablation only [23]. As a result, Celsion is currently sponsoring a global phase III clinical trial treating hepatocellular carcinoma patients with RF ablation and ThermoDox®. In addition, ThermoDox® is combined with superficial microwave hyperthermia for local breast cancer recurrence in ongoing phase I and II clinical trials [23].

[viii] Traditional temperature-sensitive liposome that triggers in the range between 42 ºC and 45 ºC and releases drug over around 30 minutes [22]

1.3. Magnetic Resonance Imaging

Magnetic Resonance Imaging (MRI) is an imaging modality that has gained extraordinary recognition in the clinic. The imaging technique allows to image soft-tissues in a non-invasively way with high contrast.

Contrast in MR images is usually caused by the proton relaxation times of mostly water protons, as well as proton density and protein content. The differences in the relaxation times of these protons give rise to the contrast in magnetic resonance (MR) images. The intrinsic relaxation times of the tissue water depend on the physiological environment. In pathological tissue this parameter may be altered [29]. When tissue protons are subjected to an external magnetic field, B_0, a net magnetization, M_0, will arise as a consequence of the imbalance in the number of spins aligning with and against the external magnetic field.

A radio frequency (RF) pulse can be used to disturb the equilibrium magnetization. When the RF pulse is turned on for a certain time until the net rotation of the magnetization vector is 90°, the net magnetization is only present in the transversal plane, M_{xy}. After excitation the spin system returns to the equilibrium by a process called relaxation. Two mechanisms that are involved are the longitudinal and the transversal relaxation, T_1 and T_2 relaxation, respectively. In longitudinal relaxation, the spins realign with the static magnetic field. This process can be described according to:

$$M_z = M_0\left(1 - e^{-\frac{t}{T_1}}\right) \tag{1.1}$$

were M_z is the longitudinal magnetization that recovers after a time point, t, in a material with a relaxation constant T_1.

While this process is taking place, transverse relaxation (or decay), the magnetic fields of individual spins interact with one another causing the spins to lose phase coherence leading to transverse magnetization decay:

$$M_{xy} = M_0 e^{-t/T_2} \tag{1.2}$$

were M_{xy} is the transverse magnetic moment at time, t, for a sample that has M_0 transverse magnetization at $t = 0$. T_2 is the transversal relaxation time [30].

1.3.1. MRI Contrast Agents

MRI contrast agents have the capacity to reduce the relaxation times of water protons in their vicinity. Most clinically used contrast agents are small molecular weight compounds that contain gadolinium (Gd) or Iron (Fe) as their active element. Both elements have electron spins that are unpaired.

The effectiveness of an MRI contrast agent is expressed in terms of relaxivity [31]. The contrast agent is better when the relaxivity is higher. The T_1 relaxitivity (r_1) is described by the formula:

$$\frac{1}{T_1} = \frac{1}{T_{1,0}} + r_1 * [CA] \tag{1.3}$$

were $[CA]$ is the concentration of the contrast agent in mM, T_1 is inverse longitudinal relaxation time in the presence of the contrast agent and $T_{1,0}$ is the inverse longitudinal relaxation time in the absence of the contrast agent. Identically T_2 relaxivity (r_2) can be calculated using T_2, and $T_{2,0}$.

There are two kinds of MRI contrast agents which can be discerned based on their r_2 over r_1 ratio. When to the r_2/r_1 is small, the CA will induce a signal enhancement, a "positive contrast" in T_1-weighted MR images. In the other hand, when a CA acts predominantly on T_2 relaxation that will result in signal reduction, a "negative contrast" in T_2-weighted MR images [32], Figure 7.

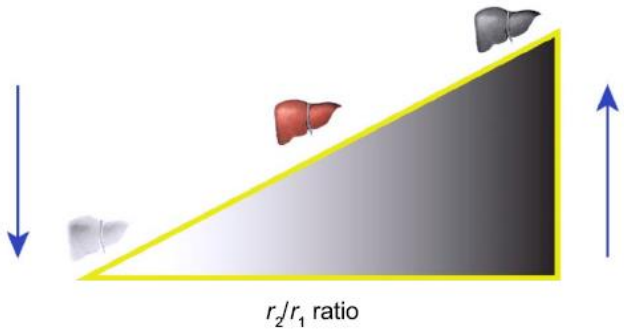

Figure 7. *Influence of the ratio r_2/r_1 on the efficiency of a contrast agent. High values of the ratio r_2/r_1 are specific for T_2 contrast agents. Figure from [32].*

1.4. MR Image-Guided Drug Delivery

Several solid tumors display poorly perfused areas [33] and often inadequate vessel formation. Consequently, some (areas within) tumors cannot be reached by the chemotherapeutic agent, leading to incomplete tumor treatment. Usually, this only can be observed by monitoring the tumor growth and/or regression over time which is a slow process. There was a need to assess the efficiency of the treatment right away so contrast agents (CAs) were encapsulated in drug-loaed TSLs. Since paramagnetic CAs happen to be less effective when they are encapsulated inside liposomes, it is possible to monitor the CA release from the liposomes and therefore indirectly also drug delivery because the reason paramagnetic CAs are less effective when encapsulated in a liposome is that the lipid bilayer restricts the number of protons that can access the CA [34], resulting in an apparently decreased ionic relaxivity. After release from the liposomes the ionic relaxivity of the CA is restored, which will create a contrast change in T_1-weighted MR imaging. It has been shown by Viglianti et al. [35] that the change of the longitudinal relaxation rate R_1 ($R_1=1/T_1$) scales with the extent of released drug in the tumor. That will be used for MR-based quantification of the temperature induced drug delivery.

The MR signal enhancement by co-release of the MRI CA and the drug enables a real time and in situ measurement for drug release, which can be called as “chemodosimetry” or “dose painting”, when referring to MRI-based drug quantification. In order to deliver the drug in an accurate way a T_1-map previous to the drug delivery is essential.

TSLs encapsulating both doxorubicin and manganese (Mn^{2+}) were earlier reported and investigated for MR image-guided drug delivery purposes *in vivo* [36]. One of the advantages of this approach is that Mn^{2+} forms a non-covalent dimer with doxorubicin inside the liposomes. This will lead to a decrease in the longitudinal relaxivity, r_1. After the release from the liposomes the Mn^{2+} interacts with negatively charged phospholipids in the tissue which will lead to an increase in r_1. Even though the CA Mn^{2+} was the first one proposed for use in image guided drug delivery, its cellular toxicity is a major advantage, which slowed down the development of Mn^{2+}-based CAs. Alternatively, Negussie et al. studied the temperature-dependent release kinetics, *in vitro,* in buffer, plasma and gel phantoms of imageable TSLs (iTSLs) encapsulated with doxorubicin and [Gd(HPDO3A)(H_2O)] [37]. *In vivo*, a MR signal increase was detected after iTSLs injection in combination with Magnetic Resonance-guided High Intensity Focused Ultrasound. De Smet et al. also studied [Gd(HPDO3A)(H_2O)] and doxorubicin encapsulated in TSLs. In Figure 8 can be seen that the r_1 of the contrast agent is apparently low caused by limited water exchange across the liposomal membrane. After release at T_m the r_1 was recovered. While cooling the r_1 became similar to the T_1-relaxivity of Gd^{3+}. This last value can be taken as experimental evidence for the quantitative release of the MRI contrast agent from the TSLs [38]. In vitro studies shows a similar release profile for both doxorubicin and Gd^{3+} [39].

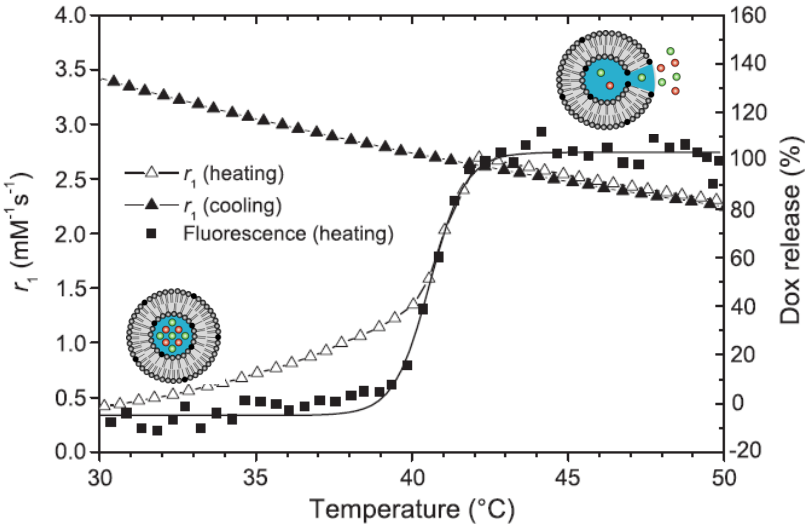

Figure 8. *Longitudinal relxivity (r_1) and doxorubicin release of TSLs in HBS during a linear temperature increase (0.5 ºC/min) from 30 ºC to 50 ºC and cooling back to 30 ºC, adapted from [38].*

1.5. Temperature-Induced Drug Delivery using MR-HIFU

The initial concept proposed by Yatvin and Weinstein [13,14] regarding hyperthermia-triggered drug delivery using TSLs was extensively evaluated in a preclinical way with different heating sources such as needle-based RF, water baths, light sources, or catheters. These methods presented drawbacks as a lack of spatial and temporal accuracy and/or limited penetration depth.

MR-HIFU, Magnetic Resonance-guided High Intensity Focused Ultrasound [40,41] embraces a great promise for the application of hyperthermia in a non-invasive, localized and controlled manner. It is an emerging technology to apply accurate deep local thermal therapies in oncology.

In order to be able to translate this technology to the clinic there was the need to improve focal heating of the tissue in a controlled way.

HIFU is applied by a phased array ultrasound transducer using an electronic beam steering developed for local hyperthermia and ablation of pathological tissue. The therapeutic ultrasound transducer focuses the ultrasound into a small focal volume at the specific target locations inside the body. The fast heating minimizes heating losses minimizing damage to healthy surrounding tissues [42]. HIFU can be combined with MRI since it has a good spatial resolution for soft tissues as well as the possibility to acquire 3D temperature information. The MRI system is responsible for planning the treatment and for providing spatial and temperature feedback while HIFU heats the tissue via an ultrasound transducer embedded in the patient table of the MR scanner.

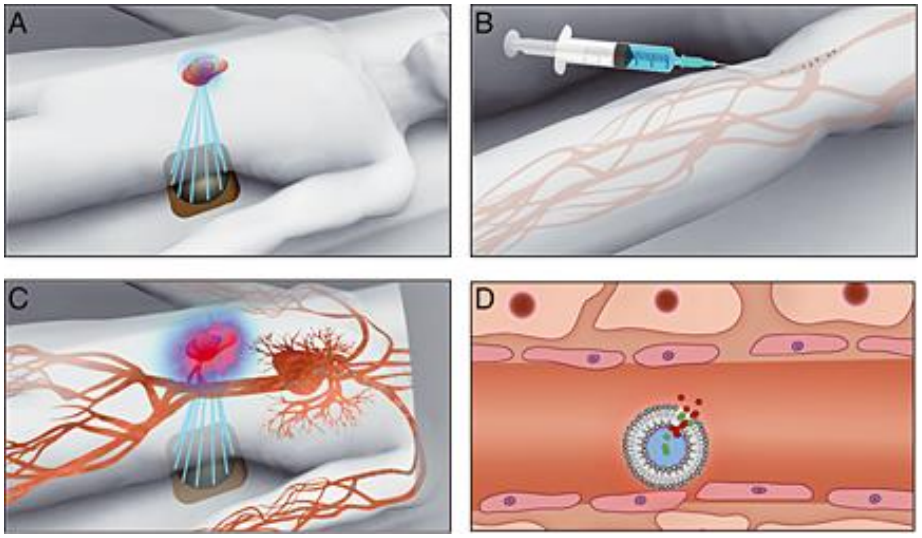

Figure 9. *Representation of temperature-induced drug delivery using MR-HIFU in combination with TSLs that encapsulate drugs and MRI CAs. In picture A is shown the MRI-guided HIFU –induced hyperthermia of a localized tumor; in picture B the intravenous injection of the liposomes that are sensitive to temperature; in picture C and D the beginning of the localized release of drug and MRI contrast agent from the TSLs. The co-release of the CA enables the estimation of the local drug delivery using MRI. Figure from [43].*

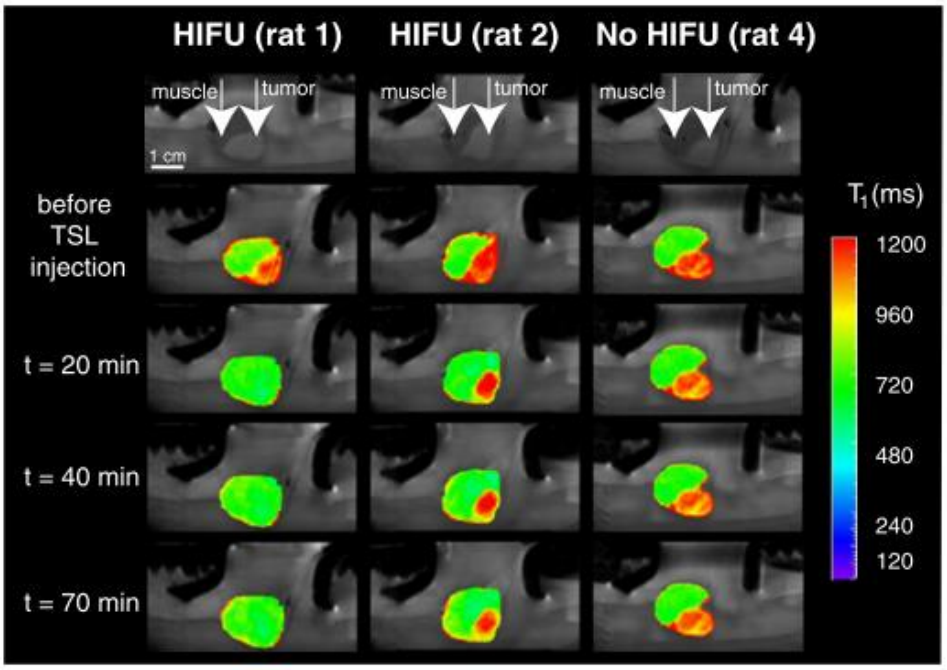

Figure 10. *In vivo MRI-guided HIFU in order to monitor local drug release. Here are shown the anatomical MR images of tumor bearing rats in the small animal HIFU setup (first line) and T_1 maps of the tumor and leg overlaid on the anatomical images at different time points. In the left column the HIFU treated tumor shows a large T_1 response; in the middle column the HIFU treated tumor showed a less sensitive response; in the right column no HIFU was performed. Picture from [38].*

MR-HIFU is used clinically for thermal ablation of uterine fibroids and for palliative treatment of bone metastasis. This technology has however potential application in temperature-induced local drug delivery at mild hyperthermia [12]. At around 42 ºC the TSLs release their content. By co-encapsulation of both a drug and a paramagnetic MRI contrast agent in the lumen of the TSLs this technique was extended to MR image-guided drug delivery using HIFU [12]. The idea of hyperthermia-triggered drug delivery from TSLs with the use of MRI-guided HIFU is illustrated in Figure 9, as well as in Appendix I.

Studies regarding hyperthermia-triggered drug delivery [44] have demonstrated the efficacy of this method. A recent study using temperature-triggered drug delivery using MR-HIFU and paramagnetic TSLs in rats bearing a subcutaneous 9L glioblastoma tumor was carried out by Smet et al., Figure 10 [38]. In this study TSLs encapsulating [Gd(HPDO3A)(H_2O)] and dox were injected at a dose of 5 mg dox/kg and the tumors were subjected to HIFU mediated hyperthermia. As it can be seen in Figure 10 a decrease in T_1 across the tumor is achieved for HIFU-treated tumors which demonstrate a release of the MRI CA from the TSLs. Otherwise in non-heated tumors T_1 only slightly decreases in the presence paramagnetic TSLs. In Figure 11, a correlation is presented between the ΔR_1, the uptake of doxorubicin and the gadolinium concentration in the tumor [38].

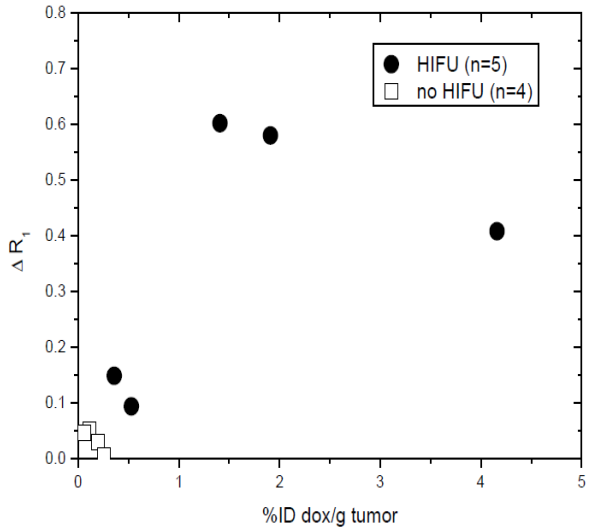

Figure 11. *On the left MR images of a gel phantom containing TSLs. Temperature maps during hyperthermia with a sonication volume with a diameter of 4 mm (A) and 12 mm (B), R_1 maps after HIFU treatment with sonication volume with d = 4mm (C) and d = 12 mm (D). Figure from [38]. On the right doxorubicin concentrations plotted against ΔR_1 for the tumors of the HIFU-treated (black circles) and HIFU-non-treated (white squares) rats injected with TSLs. Figure from [45].*

2. Research Objectives

So far, Gadolinium (Gd) and Manganese (Mn)-based CAs have been used to monitor doxorubicin release. A schematic representation of this approach is shown in Figure 12, when using Gd as a CA. Both of these MRI contrast agents pose potential health risks and therefore TSLs-based image-guided drug delivery has so far been limited to preclinical research.

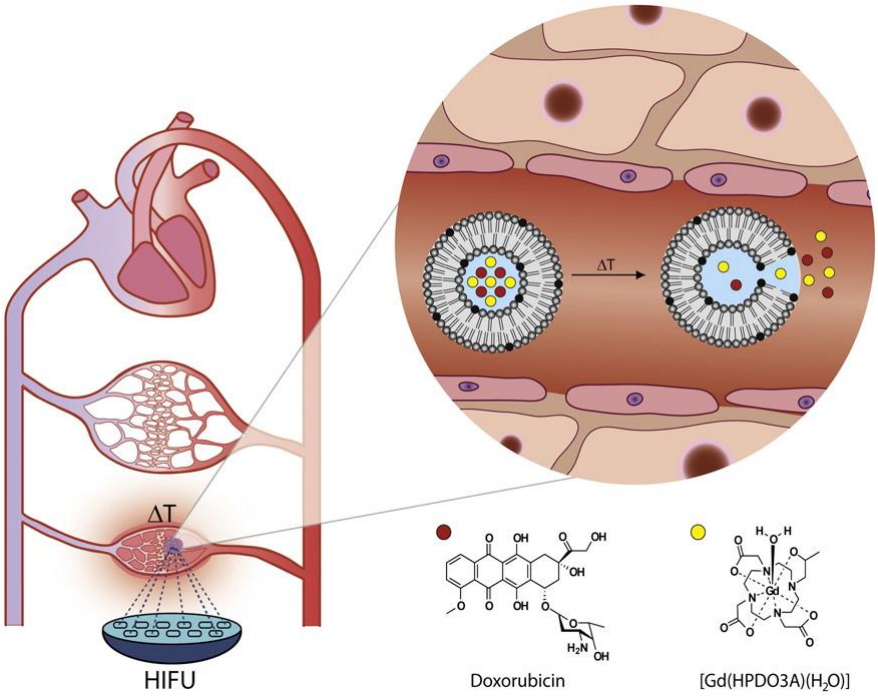

Figure 12. *Schematic representation of temperature-induced release of the drug, doxorubicin, (red dots) and the CA, [Gd(HPDO3A)(H_2O)] (ProHance®), (yellow dots) from a TSL. The local hyperthermia can be achieved non-invasively with HIFU under MRI guidance. The co-release of the CA enables the visualization and quantification of drug release in a non-invasive fashion [12,38].*

As already described, the use of TSLs co-encapsulating doxorubicin and [Gd(HPDO3A)(H_2O)] under MR image guidance for HIFU-mediated drug delivery has the potential to assess the efficacy of the drug delivery to the tumor. It was shown by de Smet et al. [38] that a good correlation exists between the uptake of drug (doxorubicin), the concentration of contrast agent [Gd(HPDO3A)(H_2O)] (ProHance®) and the ΔR_1 (longitudinal relaxivity of the contrast agent) in the tumor. As long as Gd-based MR CAs (including ([Gd(HPDO3A)(H_2O)])) are chelated they are quickly cleared by the kidney. Nevertheless patients that suffered from severe renal impairment have developed nephrogenic systemic fibrosis (NSF) [46]. It has been hypothesized that this disease is caused by the presence of free Gd^{3+} ions that are toxic and may be deposited as insoluble salts in bones, liver and spleen which lead to long-term retention of Gd^{3+} [47]. The encapsulation of [Gd(HPDO3A)(H_2O)] in the liposomes will lead to liver and spleen clearance instead

of renal clearance that happens with the free contrast agent. Because of this difference the encapsulated contrast agent will be retained longer in the body leading to doubts regarding the safety of using it in the clinic. A safer alternative MR-contrast agent is paramount to pave the way for the introduction of image-guided drug delivery in the clinic.

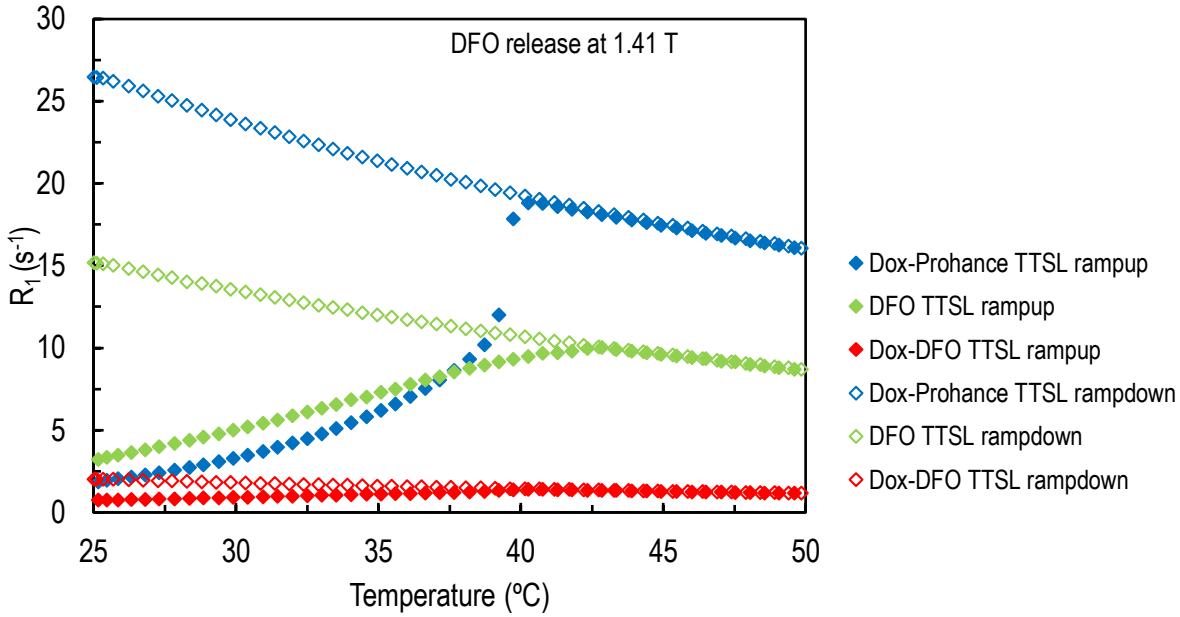

Figure 13. *Inverse T_1-relaxation times (R_1) of liposomes during temperature increase (0.5 ºC/min) from 25 ºC to 50 ºC probed at 1.41T. TTSLs encapsulating Fe-DFO (green), TTSL encapsulating Fe-DFO and doxorubicin (red) and TTSL encapsulating [Gd(HPDO3A)(H2O)] and doxorubicin (blue) as a control [48]. Fe-DFO in TTSL (green) did not release the contrast agent at a specific T_m, as required for image-guided drug delivery instead the contrast agent was released gradually under heating. TTSLs encapsulating Fe-DFO and doxorubicin (red) showed a reduced R_1 probably due to iron oxide formation or an association between iron and doxorubicin. The relaxivity of Fe-DFO was not recovered during cooling maybe because doxorubicin interacts with Fe^{3+} either by chelation of Fe^{3+} or by triggering the formation of iron oxides.*

Trying to overcome the limitations above mentioned the research group moved to a different approach, an alternative MR-imageable liposome. The contrast agent Fe^{3+}-deferoxamine (Fe-DFO) has a lowerT_1 relaxivity when compared to the CA Gd and deferoxamine (DFO) is clinically approved as an iron-chelating agent to treat patients with iron-overload. When a Fe^{3+} atom is introduced into the chelate, a T_1 contrast agent emerges (Fe-DFO). However, Fe-DFO contrast agent release characteristics were inferior with respect to its Gd loaded counterpart. The release of the contrast agent was expected to happen quickly at a specific melting phase temperature, T_m, however, for Fe-DFO the release happened gradually (Figure 13, green). The main cause can be related to the hydrophobicity of the Fe-DFO complex (Figure 14, right) allowing it to cross the bilayer or its association with the bilayer. Furthermore co-encapsulating the drug and Fe-DFO in the same liposome abolished the Fe-DFO T_1 relaxivity (Figure 13, red), possibly

due to the iron oxide formation or iron-dox aggregations [48], Figure 15. Another downside of the Fe-DFO loaded TTSL is the requirement for a low pH of the intraliposomal buffer in order to achieve stable encapsulation of the complex inside the liposome. This could lead to hydrolysis of the lipid bilayer, limiting the shelf-life of the resulting product.

To tackle these problems, a new liposome formulation will be adopted and a more hydrophilic deferoxamine-derivate (N-Suc-DFO-Fe, Deferoxamine-N-succimidyl Fe(III)), Figure 14 (left), will be used as a potential iron-based, safe MR-contrast agent with the help of NanoNextNL partner SyMo-chem. Some adaptations will be made to the previously made iron-loaded liposome. Its characteristics will be improved towards a viable option for *in vivo* drug-dose painting. These new liposomes will be characterized extensively.

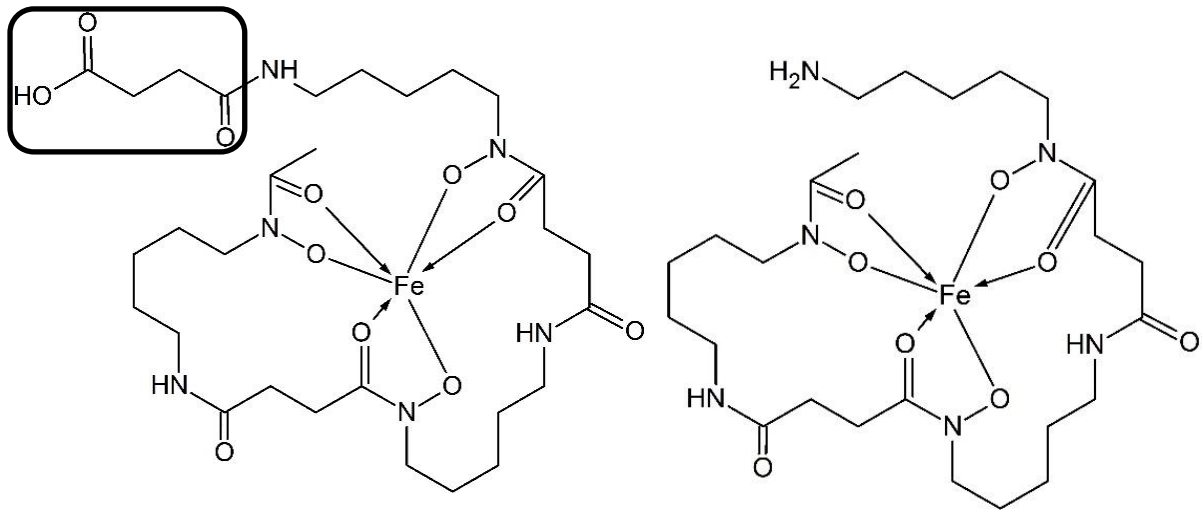

Figure 14. *Chemical structure of the new deferoxamine (DFO) variant ($C_{29}H_{49}N_6O_{11}Fe$),Deferoxamine-N-succimidyl Fe(III), obtained from SyMO-Chem BV (Eindhoven), and the previous deferoxamine mesylate ($C_{25}H_{48}N_6O_8.CH_3SO_3H$) complex, obtained from Abcam Biochemicals®, already used in a previous study.*

The aim of this project is the development and characterization of TSLs loaded with an iron-based T_1 CA. A previously investigated Fe-DFO loaded TTSL did not show all of the required characteristics for effective MR-imaging of drug delivery from TSLs. Therefore, some adaptations were made to this previously investigated system. First of all, drug-loaded liposomes will be co-injected with CA-loaded liposomes instead of co-encapsulating both drug and CA. Second of all, the lipid formulation was varied to tune the stability and release properties of the CA-loaded liposome. Finally, the iron-based CA is slightly adapted to achieve a more stable encapsulation.

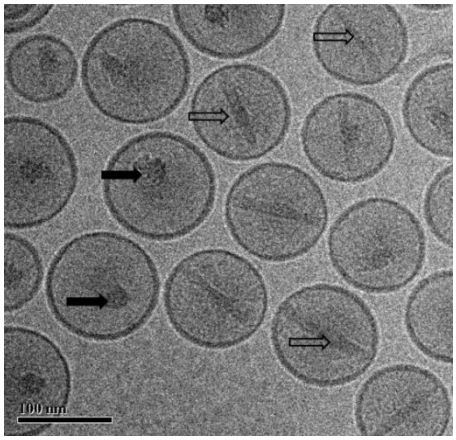

Figure 15. *Cryogen transmission electron microscopy (cryo-TEM) of TTSLs encapsulating Fe-DFO and doxorubicin. Doxorubicin crystals (open arrows) and iron oxides clusters (filled arrows) were observed, adapted from [48].*

3. Materials and Methods

3.1. Chemical Materials

1.2-Dipalmitoyl-*sn*-glycero-3-phosphocholine (DPPC), 1.2-distearoyl-sn-glycerophosphocholine (DSPC) and dipalmitoyl-*sn*-glycero-3-phosphoglyceroglycerol (DPPGOG) were obtained from Corden Pharma (Switzerland LLC).

Hydrogenated-*L*-*α*-phosphatidylcholine (HSPC), Cholesterol (CHOL) and 1.2-dipalmitoyl-*sn*-glycero-3-phosphoethanolamine-N-[methoxy(polyethyleneglycol)-2000](DPPE-PEG2000) were purchased from Avanti Polar Lipids. Chemical structures of all lipids can be seen in Appendix II.

Deferoxamine mesylate was purchased from Abcam plc (UK) and iron(III)chloride hexahydrate ($FeCl_3.6H_2O$) was purchased from Sigma Aldrich (USA), Figure 16.

Deferoxamine-N-succimidyl Fe(III) complex (DFO-N-suc-Fe(III)complex) was provided by SyMo-Chem (The Netherlands), Figure 17.

Doxorubicin hydrochloride, citrate, HEPES, chloroform, methanol, were purchased from Sigma Aldrich (USA).

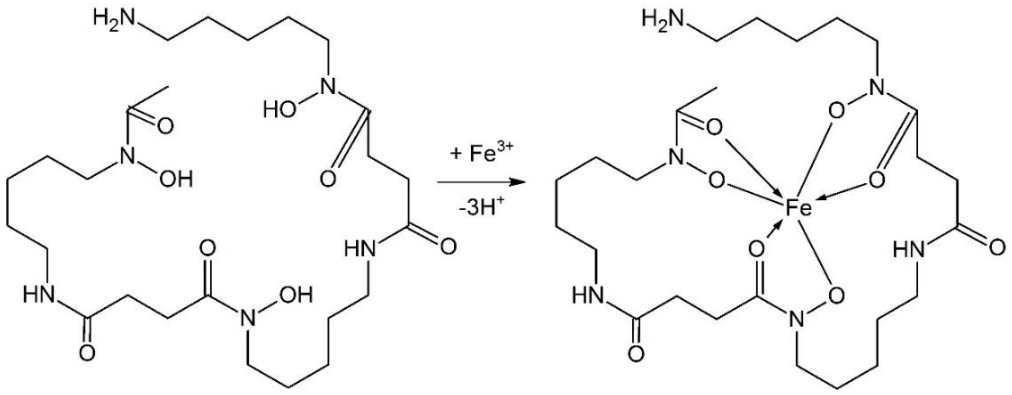

Figure 16. *Deferoxamine on the left and Iron-deferoxamine complex on the right.*

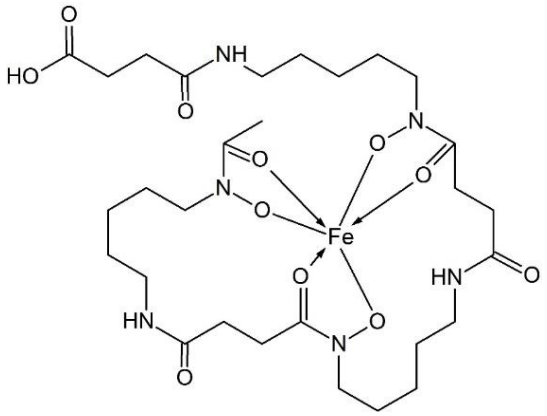

Figure 17. *Deferoxamine-N-succimidyl Fe(III) complex (DFO-N-suc-Fe(III)complex).*

3.2. Synthesis of Liposomes

Two different types of liposomes were prepared; TTSLs composed of DPPC:HSPC:Chol:DPPE-PEG2000 = 50:25:15:3 (molar ratio) and DPPGOG-TSLs composed of DPPC:DSPC:DPPGOG = 50:20:30 (molar ratio).

Using these two liposome types, five different formulations with different intraliposomal buffers and HBS as extraliposomal buffer (pH 7.8) were investigated; doxorubicin loaded DPPGOG-TSLs (containing phosphatidylglyceroglycerol, DPPGOG), doxorubicin loaded TTSLs, Fe-DFO (Deferoxamine-chelated Fe^{3+}) loaded DPPGOG-TSLs, Deferoxamine-N-succimidyl Fe(III) loaded DPPGOG-TSLs and Deferoxamine-N-succimidyl Fe(III) loaded TTSLs.

Liposomes were prepared by the film hydration and extrusion method. A lipid film was created by dissolving the lipids in chloroform:methanol (7:3 v/v). For Dox loaded liposomes, the lipid film was hydrated by $(NH_4)2SO_4$ buffer pH 5.4 or by citrate buffer pH 4. For deferoxamine Fe(III) loaded liposomes, the lipid film was hydrated by HBS pH 7.8 or acetate buffer pH 4. For deferoxamine-N-succimidyl Fe(III) loaded liposomes, the lipid film was hydrated by Gly-Gly buffer pH 8.5 or Trizma buffer pH 8.

The suspension was extruded at 60°C using a thermobarrel extruder. Samples were extruded successively through polycarbonate filters of 200 nm (two times), 100 nm (six times) pore size.

For Dox loaded liposomes, the resulting liposome solution was brought onto a PD-10 column and eluted with HEPES buffer pH 7.8, after which a solution of dox in HBS pH 7.8 (2 mg/mL or 5 mg/mL) was added to the liposomes in a at a phospholipid to doxorubicin molar ratio of 20:1. The liposomes were incubated overnight at 37 ^{o}C, after which they were passed through a 0.22 µm syringe filter. Free doxorubicin was removed using a PD-10 column. The liposomes were then concentrated using an Amicon Ultra-15 centrifugal filter unit (100 kDa MWCO, Millipore).

For the deferoxamine-N-succimidyl Fe(III) loaded liposomes, the liposomes were washed in HBS pH 7.8 using Amicon Ultra-15 centrifugal filter unit (100 kDa MWCO, Millipore). The liposomes were passed through a PD-10 column to get rid of any residual free deferoxamine-N-succimidyl Fe(III) and were re-concentrated using a Amicon Ultra-15 centrifugal filter unit (100 kDa MWCO, Millipore).

An elaborate explanation of this protocol explaining the synthesis of liposomes can be found in Appendix III.

3.3. Characterization of Liposomes

3.3.1. Fluorescence Spectroscopy

Fluorescence spectroscopy was used to determine the doxorubicin concentration and quantify the release of the drug from the liposomes (doxorubicin loaded DPPGOG-TSLs and doxorubicin loaded TTSLs).

The fluorescence measurements were performed on a Perkin Elmer LS55 Fluorescence Spectrometer (λ_{ex} = 485 nm and λ_{em} = 590 nm). All samples measured were prepared by diluting the liposomes in HBS or FBS. The liposome dispersion and a temperature probe were placed in a quartz cuvette. Then, the cuvette was positioned in the spectrometer and the dispersion stirred magnetically. The temperature of the sample was controlled by a water bath. Based on the doxorubicin loading protocol of de Smet et al. [39] the proportion between doxorubicin and lipids was estimated to prepare calibration lines with concentrations in the same order of magnitude.

The release of the drug from the liposomes was probed by means of fluorescence measuring the intensity of fluorescence as a function of temperature. The release of doxorubicin from the liposomes (15 µL) in preheated HBS (2.185 mL) was determined at 37 ºC or 42 ºC. At the end of each measurement 5 µL of a 10 % v/v solution of Triton X-100 was added to 2.2 mL of the solution in order to afford quantitative release of the drug doxorubicin. The percentage of doxorubicin released was calculated according to:

$$\frac{I_t - I_0}{I_{100} - I_0} x\ 100\ \% \tag{3.1}$$

In which I_t is the intensity of the fluorescence at a specific time (t), I_0 is the intensity of the fluorescence at $t = 0$ and I_{100} is the intensity of the fluorescence after adding Triton X-100.

The intraliposomal doxorubicin concentration was determined fluorimetrically after destruction of the liposomes with Triton X-100. The intensity of all samples were measured at room temperature.

3.3.2. Inductively Coupled Plasma (ICP)

Inductively Coupled Plasma-Optical Emission Spectrometry (ICP-OES) is a very sensitive analytical technique used for detection of trace metals in a myriad of sample types [49]. This approach is a type of emission spectroscopy that is based in the spontaneous emission of photons (at wavelengths characteristic of a particular element) from atoms and ions that have been excited in a radio-frequency (RF) discharge [50]. The specific intensity of the emission will indicate the concentration of the element in the sample.

Phosphorus and iron concentrations were determined by means of ICP-OES. The samples were submitted in glass tubes and acid was added to the samples. The samples are then destructed using a heating block. When the destruction is completed the samples are cooled down and diluted to a certain known volume. The amount of iron (Fe) and phosphorus (P) present in the sample are determined using ICP-OES. During this analysis the sample solutions are fed through a nebulizer. This will generate an aerosol which is led into an argon plasma. Already in this plasma the solution is evaporated, atomized, excited and ionized, that will produce element-specific emission. In the course of ICP-OES analysis, the intensity of the emission is being used to define the amount of Fe and P present in the sample. In order to control the quality blanks are taken along the analysis. Each blank, calibration standard and sample solution contains corresponding amounts of internal standard to correct for system variations during measurement. Each ICP measurement involves multiple replicates and each element is measured using multiple wavelengths.

3.3.3. Dynamic Light Scattering (DLS)

Dynamic Light Scattering (DLS) is sometimes referred as Photon Correlation Spectroscopy or Quasi-Elastic Light Scattering. This is a technique to measure the size of particles usually in the submicron region. DLS measures Brownian motion and relates it to the size of the particles. The velocity of this motion is defined by the translation diffusion coefficient.

For characterization of the liposomes the mean particle size and polydispersity index (PD.I) were evaluated with DLS (DLS; ALV/CGS-3 Compact Goniometer System, ALV-GmbH, Langen, Germany). The PD.I is a dimensionless measure of the broadness of the size distribution calculated from the

cumulants analysis. Intensity correlation functions were measured at a scattering angle of θ = 90º using a wavelength of 632.8 nm. The translation diffusion coefficient (D) was obtained from cumulant fits of the intensity correlation function using AVL software. All stated hydrodynamic radius were calculated using the Stokes-Einstein equation:

$$r(H) = \frac{kT}{3\pi\eta D} \tag{3.2}$$

where k is the Boltzmann's constant, T is the absolute temperature and η is the viscosity of the solvent [51]. The temperature of the sample is part of the AVL-Goniometer System and is precise to approximately ± 0.1 ºC absolute and ± 0.1 ºC relative [52].

Between 0.5 µL and 10 µL of sample were diluted in 2 mL of filtered HEPES buffered saline at pH 7.8. The liposome formulation was measured 5 times for 10 seconds.

3.3.4. Differential Scanning Calorimetry (DSC)

Calorimetry is a technique for measuring the thermal properties of materials in order to create an association between temperature and specific physical properties of substances [53]. Amongst several types of calorimeters, differential scanning calorimeter (DSC) is a popular one. This is a thermo-analytical technique that measures the differences in amount of heat required to increase the temperature of a sample as a function of temperature. It is based on physical transformations that require more or less heat flow, dependent if the process is endothermic or exothermic.

The phase transition temperatures of the lipid membranes were determined with differential scanning calorimetry (Q2000 differential scanning calorimetry, TA instruments, USA).

After enclosing 10 µl of suspension into a T-zero hermetic pan, the pan is loaded into the DSC (at 20 ºC) for analysis. During analysis, the sample is heated, cooled and heated again from 20 ºC to 60 ºC, using a heating rate of 5 ºC /min; the melting temperature of the liposomes is determined during the second heating cycle.

To obtain accurate results at these relatively low temperatures, an ultra-pure Gallium reference is analyzed and used to correct the liposome melting temperature as analyzed by the DSC.

3.3.5. Cryo-Transmission Electron Microscopy (cryo-TEM)

Morphology was determined by cryogen transmission electron microscopy (Cryo-TEM). Sample preparation was performed by applying a 3 µl droplet of suspension to a lacey carbon film and subsequently plunge-freezing this sample into liquid ethane using a Vitrobot. As a result, an amorphous ("vitrified") ice film is created, containing the particles of interest. Subsequently, cryo-TEM studies were performed using a FEI TECNAI F30ST (300 kV, using a cryo-holder, keeping the samples temperature at -170 °C during the studies). Imaging was done in low-dose mode on a CCD camera (1 k x 1 k). For several locations on the sample, images were acquired at under-focus conditions.

3.3.6. Nuclear Magnetic Resonance Spectroscopy

The release of deferoxamine Fe(III) and deferoxamine-N-succimidyl Fe(III) complex from the liposomes were studied by measuring the longitudinal relaxation time, T_1, as a function of the temperature at 60 MHz, 1.41 T (Minispec MQ60, Bruker, Germany, Magnet Temperature = 40 ºC). A standard spectroscopic inversion recovery NMR sequence was used (four scans per data point, ten data points for fitting and the recycle delay and final pulse separation were adjusted appropriately for each individual sample). TSL samples (180 µL, around 5 mm tall in Bruker glass NMR tubes 180 mm x 7.5 mm x 0.6 mm) were prepared in HBS or in FBS. The experiments were performed from 23.0 ºC to 52.0 ºC (heating rate = 0.25 ºC/min), followed by cooling down from 52.0 ºC to 23.0 ºC (- 0.25 ºC/min). The longitudinal relaxivity (r_1) can be calculated according to:

$$r_1 = \frac{\frac{1}{T_1} - \frac{1}{T_{1,0}}}{[Fe]} \tag{3.3}$$

were T_1 is the longitudinal relaxation time, $T_{1,0}$ is the longitudinal relaxation time of the HBS buffer, and $[Fe]$ is the concentration of deferoxamine Fe(III) or deferoxamine-N-succimidyl Fe(III) complex (DFO-N-suc-Fe(III)complex) in mM.

Additionally the release of Fe-DFO and DFO-N-suc-Fe(III) complex from the liposomes was studied by measuring the longitudinal relaxation time (T_1) after different timespans of heating at 60 MHz (1.41 T). TSLs (20 µL) were added to preheated HBS and FBS (180 µL, T = 25, 37, 39, 41, 42 and 45 ºC). Samples were taken at several time intervals (t = 1, 5, 15, 30, 60 minutes). Each sample was directly cooled on ice and measured at 23 ºC. T_1-relaxation times were measured with an Inversion Recovery sequence (10 inversion

times 5 – 5000 ms, TR > 5 T_1, 4 averages, mono-exponential fit). Inverse T_1 relaxation times were plotted against the heating time.

The longitudinal (r_1) and transversal (r_2) relaxivities of the DFO-N-suc-Fe(III) complex liposomes and DFO-N-suc-Fe(III) complex alone were measured with a 60 MHz (1.41 T). Dilution series of the original suspensions were prepared in HBS and samples (180 µL) were measured at 37 ºC. T_1 relaxation times were measured with an Inversion Recovery sequence. T_2 relaxation times were measured with a Carr-Purcell-Meiboom-Gill sequence. Inverse T_1 and T_2 relaxation times were plotted against corresponding Fe^{3+} concentration, and the slope of the calculated linear fit provided r_1 and $r_2$respectively.

3.3.7. Water Exchange Rate Across the Lipid Bilayer

From the paramagnetic liposomal solution, the extraliposomal buffer (HBS) and the intraliposomal buffer (with Fe-DFO or DFO-N-suc-Fe(III) complex and different inner buffers), T_1 measurements were performed at 60 MHz, 1.41 T, (Minispec MQ60, Bruker, Germany, Magnet Temperature = 40 ºC), at 37 ºC. The volume fraction of the intraliposomal space f was calculated by dividing the Fe concentrations of the liposomal solutions, $[Fe]_{sol}$, by the iron concentration of the intraliposomal buffer $[Fe]_{in}$:

$$f = \frac{[Fe]_{sol}}{[Fe]_{in}} \tag{3.4}$$

The water exchange rate k_{ex} over the liposomal membrane was calculated according to the two-compartment model:

$$k_{ex} = \frac{1}{\tau_{in}} \; and \; \tau_{in} = \frac{f}{R_{1,eff} - R_{1,bulk}} - \frac{1}{R_{1,in}} \tag{3.5}$$

were k_{ex} is transmembrane water exchange rate, τ_{in} is the average residence time of water inside the liposomes, $R_{1,eff}$ is the longitudinal rate of the paramagnetic liposomal solution, $R_{1,bulk}$ is longitudinal relxation rate of the extraliposomal solution, $R_{1,in}$ is the longitudinal relaxation rate of the intraliposomal water protons and f is the volume fraction of the intraliposomal space. The parameter k_{ex} is directly correlated to the size of the studied liposomes.

3.3.8. Magnetic Resonance Imaging

Magnetic Resonance Imaging was performed at 3 T (Achieva, Philips Healthcare, The Netherlands). The T_1 and T_2 measurements on the liposomes (i.e. TTSL) containing an intraliposomal concentration of 220 mM DFO-N-suc-Fe(III) were performed at 37 ºC, in which four of the eight samples were heated for 30 min at 45 ºC. The total concentration of DFO-N-suc-Fe(III) was adjusted to 3.2, 1.6, 0.8 and 0.4 mM. The samples were placed in a sample holder containing a standard phantom solution (0.77 g/L $CuSO_4 \cdot 5H_2O$ and 2 g/L NaCl).

T_1-weighted MR images were obtained using an inversion recovery pulse sequence (TE = 7.7 ms, TR = 8.4 s, FOV = 70 mm × 70 mm, slice thickness = 4 mm, voxel size = 0.486 mm × 0.486 mm, NSA=5). A T_1 map was calculated from the T_1-weighted MR images with 12 different inversion times, varying from 50 ms until 5000 ms (50, 100, 150, 250, 500, 750, 1000, 1500, 2000, 3000, 4000, 5000 ms).

T_2-weighted MR images were obtained with a turbo spin echo sequence (TE varying from 40 ms to 1280 ms, TR = 8400 ms, FOV = 70 mm × 70 mm, slice thickness = 4 mm, voxel size= 0.398 mm × 0.398 mm, NSA = 3, TSE-factor = 32), of which a T_2-map was calculated. The average T_1 and T_2 values and standard deviations of the different samples were calculated from the pixels within a manually traced ROI.

3.3.9. Magnetic Resonance Imaging and High Intensity Focused Ultrasound on Gel Phantom

Temperature-induced release experiments were performed on gel phantoms and a clinical MR-HIFU system (Sonalleve MR-HIFU Philips Healthcare) was used. In this system the MRI is responsible for providing spatial and temperature feedback to the ultrasound transducer [12] and the HIFU transducer is embedded in the patient bed of a clinical 3T MRI scanner (Achieva 3.0 T, Philips Healthcare, The Netherlands). Gel phantoms were prepared from low gelling agarose (Sigma, Germany) (2 % w/w) and silicon dioxide (2 % w/w) and homogenously mixed with TTSLs (a more elaborate explanation of this protocol can be found in Appendix IV). The liposomes were only added to the gel when the temperature was sufficiently below the T_m in order to prevent any release while the gel was being prepared. The gel phantom was then places between gel pads in a water bath at 37 ºC above the HIFU transducer. A part of the gel was heated to 42 ºC for 15 minutes with a sonication diameter of 4 mm (20 W, 29 seconds to reach 42 ºC) or diameter of 8 mm (15W) respectively. The sonications were controlled with a binary feedback loop with a modified algorithm in order to keep the desired temperature, with the use of temperature maps [45].

The MR thermometry sequence was a single slice gradient echo sequence with the parameters: flip angle = 19.5 º; TR/TE = 50/19.5 ms; EPI-factor = 7; SENSE factor = 1.8; field of view = 250 mm × 250 mm; matrix = 176 × 169; slice thickness = 4 mm; number of averages = 4; acquisition time = 4 min, 50 s.

R_1 maps were acquired using a single slice steady state inversion-recovery Look-Locker sequence with parameters: flip angle = 10 ºC; TR/TE = 9.7/3.7 ms; interval time = 100 ms; time of inversion repetition = 6 s; EPI-factor = 5; field of view = 65 mm x 185 mm; matrix = 240 mm x 180 half scan = 76%; slice thickness = 5 mm; number of averages = 2; fat suppression = SPIR; acquisition time = 7 min, 12 s.

4. Results and Discussion

4.1. Doxorubicin Loaded in DPPGOG-TSLs

As concluded in previous work by Hummelink [48], the relaxivity was abolished when liposomes encapsulated both doxorubicin and Fe-DFO. Additionally doxorubicin doesn't get loaded at high pH values, which are required to keep the DFO-N-suc-Fe(III) complex encapsulated. Since the aim of the work would be to co-inject liposomes encapsulating the drug plus liposomes encapsulating the contrast agent instead of co-encapsulating both substances in the same liposomes, the first step was to study the release of doxorubicin from DPPGOG-TSLs liposomes. DPPGOG-TSLs are being studied instead of TTSLs since the encapsulating of Fe-DFO in TTSLs leads to a gradual release of the contrast agent instead of a quick release. Trying to tackle this problem, the lipid formulation was changed.

DPPGOG-temperature-sensitive liposomes were prepared, encapsulating doxorubicin as a drug. Doxorubicin was actively loaded into the liposomes using the citrate pH gradient. Traces of unencapsulated doxorubicin were removed using PD-10 columns.

This process yielded doxorubicin liposomes with a hydrodynamic radius of around 71 nm and a PD.I of 0.0748, Figure 18, measured with DLS.

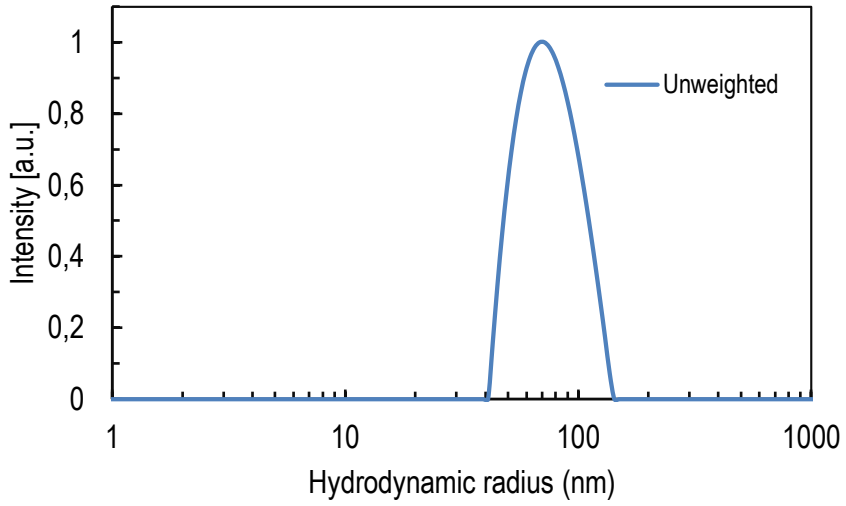

Figure 18. *Temperature-sensitive liposomes with DPPGOG were prepared encapsulating doxorubicin. This process yielded doxorubicin with a hydrodynamic radius of around 71 nm and a PD.I of 0.0748.*

The fluorescence at high doxorubicin intraliposomal concentrations is quenched. When the doxorubicin is released from aqueous interior of the liposomes the doxorubicin will be diluted in the extraliposomal buffer to concentrations below its self-quenching concentration. This will lead to an increase in fluorescence intensity. The almost instantaneous increase in fluorescence that was observed when DPPGOG-TSLs were subjected to a temperature of 42 ºC indicates full release, both in HBS and FBS, after less than five minutes, Figure 19. In addition the stability of DPPGOG-TSLs containing doxorubicin was tested in FBS and HBS. FBS release measurements were performed since it is closer to mimic the behavior *in vivo*. Leakage of below 20 % of doxorubicin at 37 ºC was observed after one hour.

In previous studies [48] the presence of Fe-DFO in the intraliposomal space reduced the loading of doxorubicin into the liposomes as free doxorubicin was observed during the loading procedure. Encapsulating only doxorubicin in DPPGOG-TSLs did not show any loading problems. The next step was to encapsulate only Fe-DFO in the same liposome formulation in an attempt to create Fe-DFO loaded liposomes with the same temperature-sensitive behavior as the dox loaded DPPGOG-TSLs.

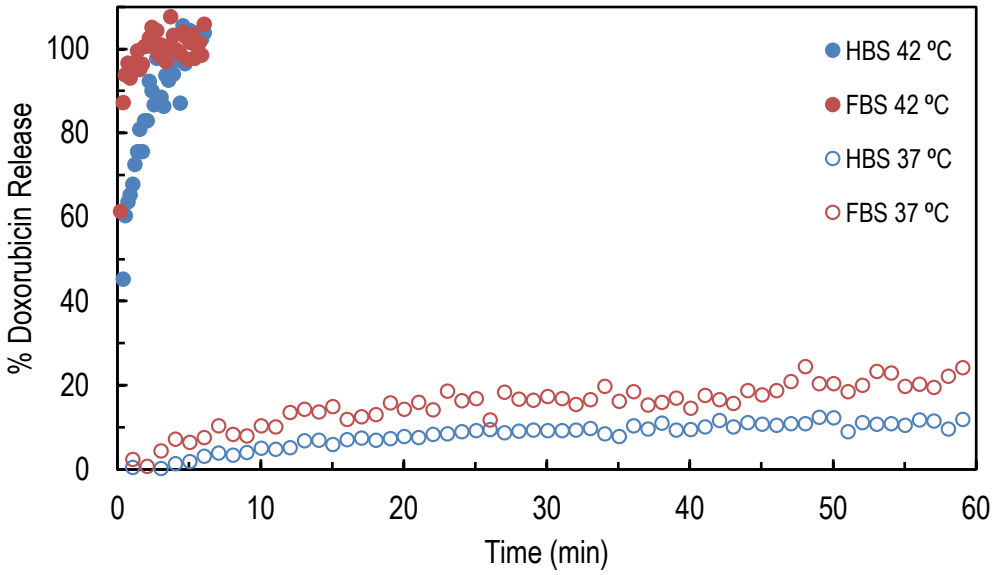

Figure 19. *Release of doxorubicin from DPPGOG-TSLs in HBS (HEPES buffered saline) and FBS (fetal bovine serum). The samples were preheated to 37 ºC and 42 ºC. The percentage of doxorubicin released was calculated from the fluorescence intensities which were measured over time.*

4.2. Deferoxamine Fe(III) Loaded in DPPGOG-TSLs

Next to DPPGOG-TSLs encapsulating doxorubicin, Fe-DFO DPPGOG-TSLs were prepared according to the procedure described in Appendix III.

In this study Fe-deferoxamine (Fe-DFO) was encapsulated in the liposomes as a MR contrast agent. This nanoparticle yields lower T_1-contrast with respect to Gd^{3+}-particles, but does not have the intrinsic problem of potential Gd^{3+} toxicity, which precluded in the past clinical translation of Gd-based nanoparticles [5,43].

Deferoxamine (DFO) is a siderophore from the bacterium *Streptomyces pilosus* and it is used as a treatment for iron overload [54]. Additionally, DFO has been often employed to chelate Fe ions for MR purposes. This approach offers an alternative to Gd-based nanoparticles for T_1-MR imaging, thereby avoiding all potential risk associated with long-term organ retention of Gd.

Fe-deferoxamine loaded DPPGOG-TSLs with acetate as intraliposomal buffer

Storage conditions

The first research objective using acetate as an inner buffer was searching the best way to store the liposomes over time. In order to investigate which storage method was best, the quality of the liposomes was assessed by measuring their hydrodynamic radius and by investigating their encapsulation stability by measuring their T_1 values over time. As depicted in Table 1, DPPGOG-TSLs should not be frozen using liquid nitrogen since both the hydrodynamic radius and the PD.I value increased. Moreover, when frozen either gradually or instantly using liquid nitrogen, the liposomes showed a T_1 drop after thawing, indicating content release (Figure 20). From the T_1 data, it could be concluded that the best way to store the liposomes is keeping them in the fridge, at 4 ºC. After the T_1 value was maintained up to 9 days at this temperature. The same formulation was reproduced with HBS as intraliposomal buffer. Some results can be seen in Appendix V.

	Hydrodynamic radius (nm)	PD.I
Room Temperature (RT)	75.06	0.0387
Gradually frozen at -20 ºC	77.82	0.0181
Instantly frozen in liquid N_2	87.35	0.1900

Table 1. *DPPGOG-TSLs encapsulating Fe-DFO and using acetate as intraliposomal buffer. When the liposomes are frozen instantly in liquid N_2 the hydrodynamic radius increases considerably but also the PD.I which can be related to the formation of aggregates. When gradually frozen at -20 ºC the size of the liposomes is maintained as well as a low PD.I value.*

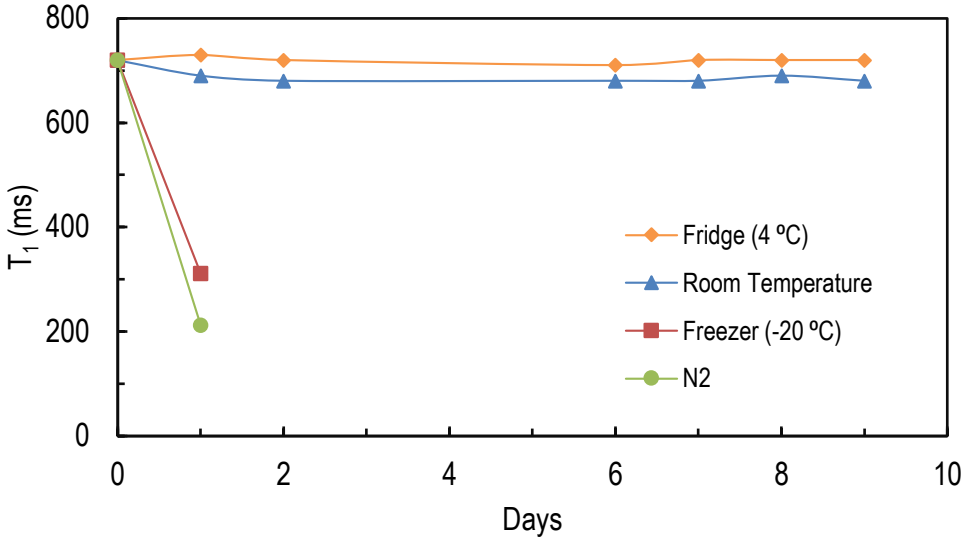

Figure 20. *T_1 measurements of liposomes overtime when four different ways of storage are considered: 4 ºC in the fridge, room temperature (RT), gradually frozen at - 20 ºC and kept in the freezer, instantly frozen with liquid nitrogen. All liposomes were kept in HEPES buffered saline, pH 7.8. NMR measurements, at 1.41 T, showed that these liposomes were leaky when frozen at - 20 ºC or with N_2.*

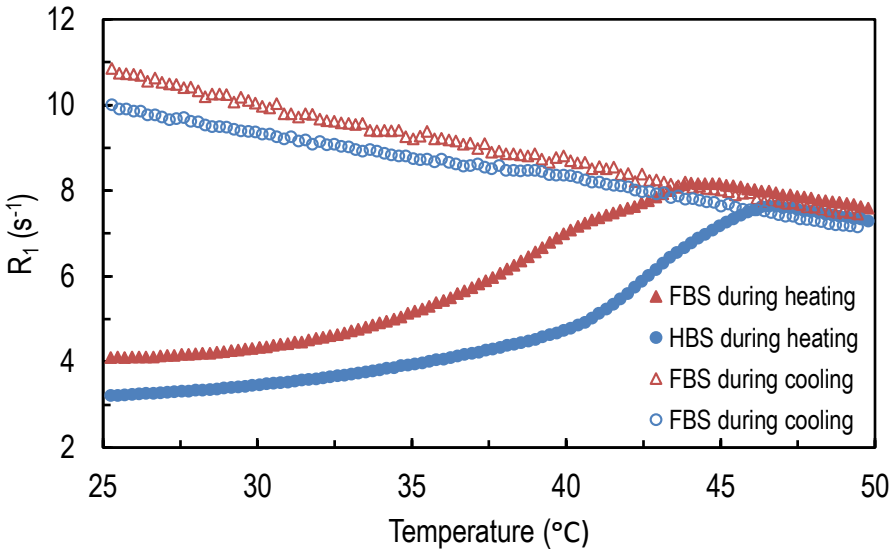

Figure 21. *Inverse T_1-relaxation times of liposomes during a linear temperature increase (0.25 ºC/min) from 23 ºC to 52 ºC, and temperature decrease, from 52 ºC to 23 ºC, probed at 1.41 T in 90 % FBS (red) and in HBS (blue).*

Fe-DFO release assays

The inverse T_1-relaxation times of the paramagnetic liposomes were studied over a temperature range of 23.0 ºC to 52.0 ºC at 1.41 T. In Figure 21 the change of inverse T_1-relaxation time as a function of temperature for Fe-deferoxamine DPPGOG-TSLs is shown in 90 % in FBS and in HBS. Liposomes behaved differently in the presence of serum proteins compared to buffer.

When the temperature increases the permeability of the bilayer to water also increases which leads to an increase in the net ionic relaxivity. A faster increase of R_1 is seen when is seen around the T_m of the membrane. This indicates that the CA gets released and thereby regains access to extraliposomal water protons. In Figure 22, in HBS, it is shown that when Fe-DFO is encapsulated in DPPGOG-TSLs instead of TTSLs a closer pattern to the heating cooling curve of gadolinium is achieved (in blue). Since a different concentration of iron and gadolinium was used the shape is the only way to compare de curves. A slope around T_m is expected and not a gradual increase. DPPGOG-TSLs encapsulating Fe-DFO released the contrast agent at a specific T_m, (and not gradually), as required for image-guided drug delivery. Although in HBS a slope can be seen around 42 ºC, full release seems to happen only around 45 ºC. This shift when compared to the T_m (41 ºC) presented by the Gd-TTSLs suggests and interaction of Fe-deferoxamine with the lipid bilayer [48].

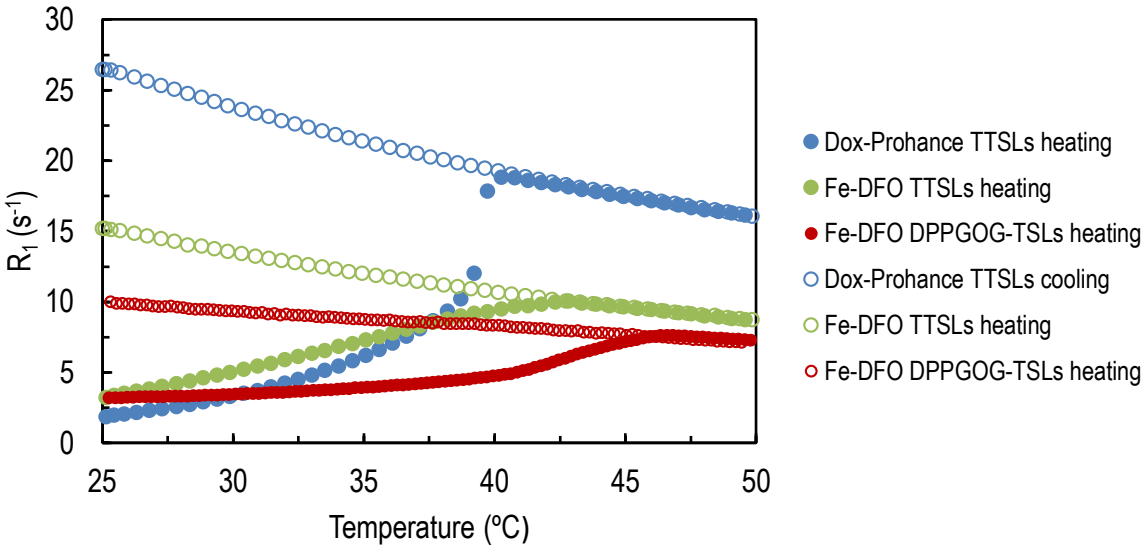

Figure 22. *Inverse T_1-relaxation times (R_1) of liposomes during temperature increase probed at 1.41T. TTSLs (Traditional temperature-sensitive liposomes) encapsulating Fe-DFO (green), DPPGOG-TSLs encapsulating Fe-DFO (red) and TTSLs encapsulating [Gd(HPDO3A)(H_2O)] (blue)I* [48].

Next, the longitudinal relaxation time (T_1) of the DPPGOG-TSLs samples was measured as a function of temperature and time, in order to study the release of the Fe-DFO from the liposomes. This resulted in the release curves presented in Figure 23. For all samples a fast release of Fe-DFO from the liposomal

carrier was observed during the first 15 minutes, reaching a constant value for all time points thereafter. The maximum release increased with increasing temperatures and reached a value at 42 ºC that corresponds to almost 100 % of release of the Fe-DFO. This behavior is in contrast to the comparable system of Fe-DFO TTSLs, Figure 24, where 100 % release is only observed at temperatures close to T_m = 45 ºC. As the aim was to develop a liposome that shows fast and quantitative release of Fe-DFO around 42 ºC, the DPPGOG-TSLs (Figure 23) were behaving more promisingly than the Fe-DFO loaded TTSLs, which were tested before (Figure 24).

Although at room temperature, the Fe-DFO was stably encapsulated in the DPPGOG-TSLs, Figure 23 (blue circles), unfortunately, at body temperature (red squares) the leakage of Fe-DFO from the liposomes is large and fast. Further optimization is needed in order to improve stability. Slightly changing the contrast agent while maintaining the DPPGOG-TSLs formulation could be an option in order to achieve this.

The release curves of DPPGOG-TSLs encapsulating Fe-DFO were measured in FBS while the release curves of TTSLs encapsulating the same contrast agent were measured in HBS, which could lead to some of the differences described. Stability tests in FBS were opted for as these experimental conditions are closer to what will be experienced *in vivo*.

By changing the liposome formulation the release was improved. The next step would be to improve the stability by slightly changing the iron-deferoxamine in order to make it charged at higher intraliposomal pH. The hypothesis is that the charge will limit the passage of the CA over the liposomal bilayer.

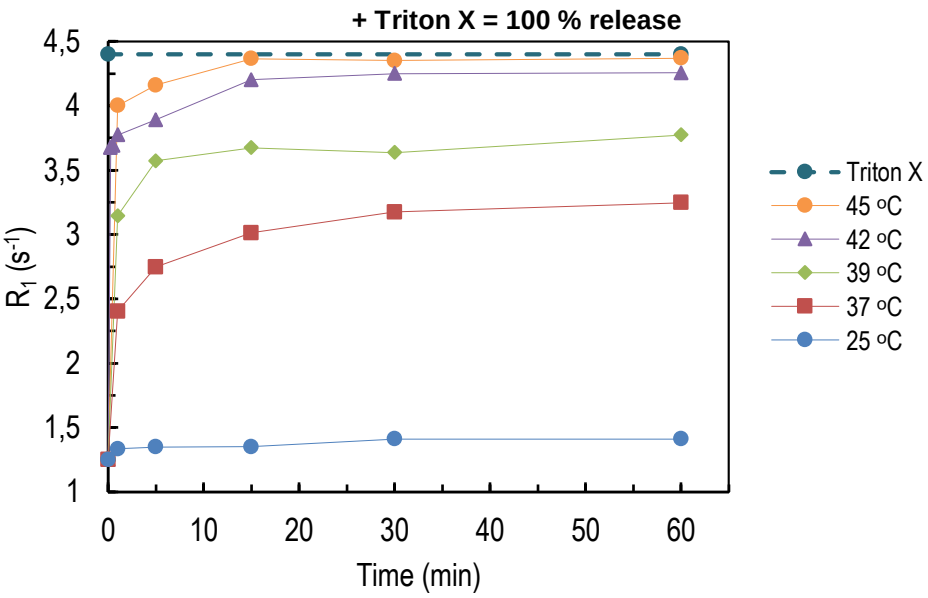

Figure 23. *Release of encapsulated Fe-DFO from the liposomal system, DPPGOG-TSLs measured at 1.41 T, in 90 % FBS.*

In order to improved stability an attempt was made by encapsulating DFO-N-suc-Fe(III) complex in the same liposomes formulation and using different intraliposomal buffers. However, this lead to either incomplete release in case of the Trizma buffer or to a failure to encapsulate the new compound inside the liposomes (when gly-gly buffer was used). The data from these experiments can be found in Appendix V.

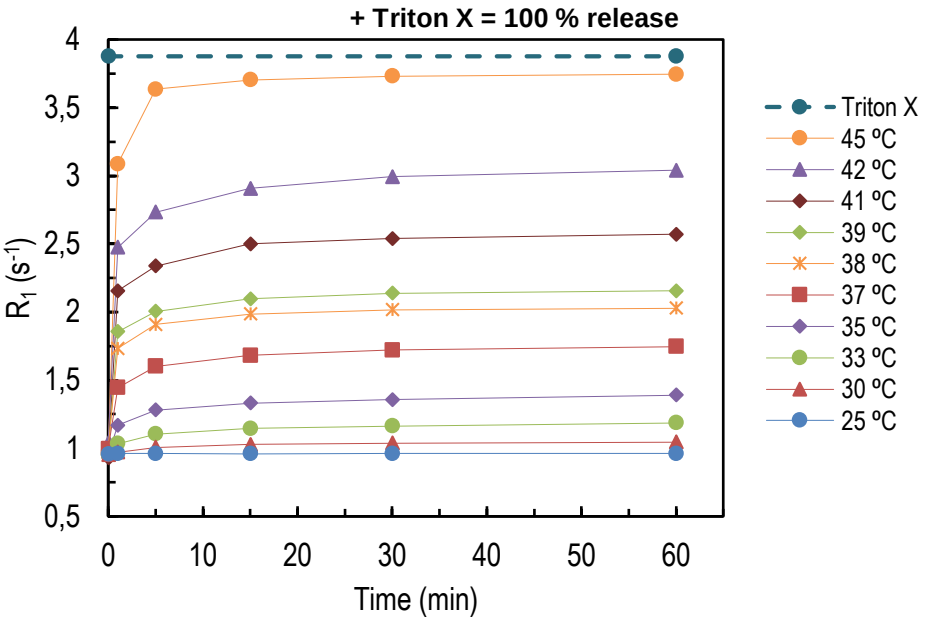

Figure 24. *Release of encapsulated Fe-DFO from the liposomal system, TTSLs measured at 1.41 T, in HBS, adapted from [48].*

4.3. Deferoxamine N-succimidyl Fe(III) Loaded TTSLs

Since some problems were experienced when DFO-N-suc-Fe(III) complex was encapsulated in DPPGOG-TSLs, TTSLs were used again, this time encapsulating DFO-N-suc-Fe(III) complex in an attempt to increase the stability of the iron-encapsulation inside the liposomes.

4.3.1. Nuclear Magnetic Resonance Spectroscopy

DFO-N-suc-Fe(III) Release Assays

The release of DFO-N-suc-Fe(III) complex from TTSLs in HBS and FBS was studied by measuring the longitudinal relaxation time (T_1) as a function of the temperature at 1.41 T. The release was monitored from 23 ºC to 52 ºC applying a constant heating rate of 0.25 ºC /min, Figure 25.

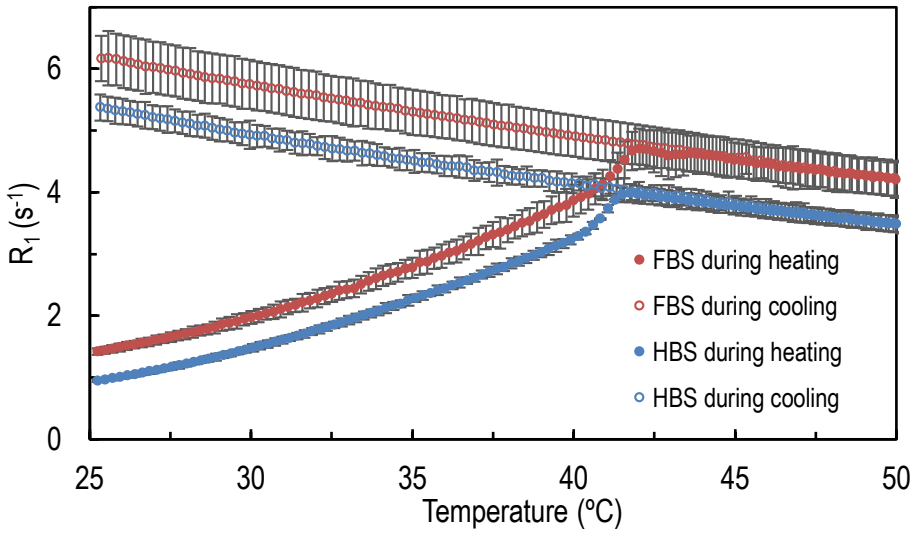

Figure 25. *Inverse T_1-relaxation times of liposomes during a linear temperature increase (0.25 ºC/min) from 23 ºC to 52 ºC, and temperature decrease, from 52 ºC to 23 ºC, probed at 1.41 T in 90 % FBS and HBS.*

The encapsulation of DFO-N-suc-Fe(III) inside the liposomes reduced the observed longitudinal relaxivity compared to free DFO-N-suc-Fe(III) as the water exchange between the bulk water outside and the DFO-N-suc-Fe(III) inside the liposomes is reduced by the lipid bilayer. Upon release from the inner lumen of the liposomes, the relaxivity of free DFO-N-suc-Fe(III) is recovered.

All NMR measurements showed an increase in r_1 (as is observed from the increase in R_1 while the Fe-DFO concentration is constant) during heating, at temperatures below the T_m (see point 4.3.5) due to an increase in water permeability of the lipid bilayer.

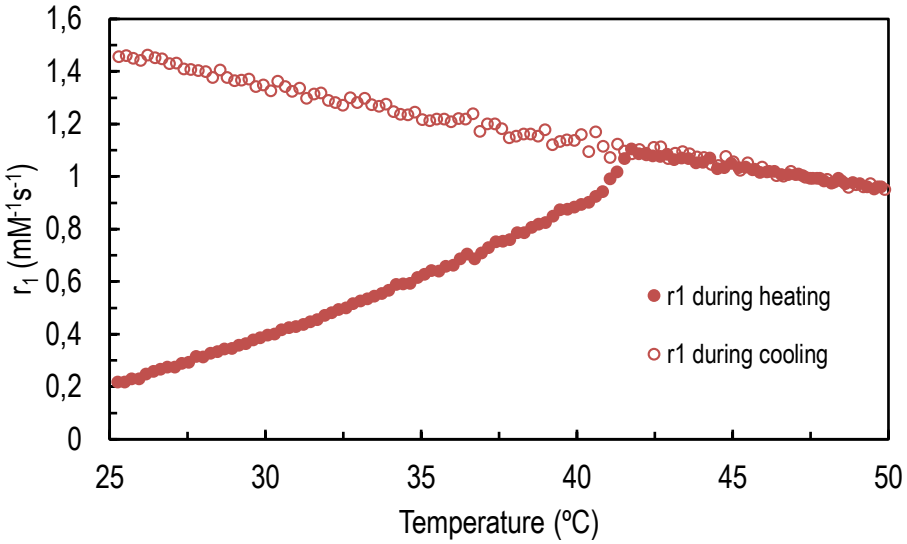

Figure 26. *The release of DFO-N-suc-Fe(III) was probed with the longitudinal relaxivity (r_1).*

A rapid increase in r_1 was observed between 41 ºC and 42 ºC. This effect was attributed to the release of DFO-N-suc-Fe(III) from the lumen of the TSLs, Figure 26. When the liposomes are heated above the T_m the relaxivity curve corresponds to the relaxivity of the free DFO-N-suc-Fe(III), as it can be seen in Appendix V. This indicates nearly full release.

In addition, the stability of TTSLs containing DFO-N-suc-Fe(III) was tested in 90% pre heated fetal bovine serum (FBS), Figure 27, and in HBS, Appendix V, at 37 ºC. The longitudinal relaxation rate (R_1) remained constant over time, indicating that no measurable release of DFO-N-suc-Fe(III) occurred at body temperature. When subjected to a temperature of 42 ºC, the formulation showed a fast increase of the R_1, indicating a fast release of DFO-N-suc-Fe(III).

In review with this formulation the stability was improved, as well as the release. In FBS, at 42 ºC, after 5 minutes, around 80 % of DFO-N-suc-Fe(III) complex was released. Although, the liposome formulation could be tuned in order to increase the release at 42 ºC, overall this liposome formulation seemed a reasonable candidate.

Relaxivity at 1.41T

Next the longitudinal (r_1) and the transversal (r_2) relaxivities of the paramagnetic liposomes and of the DFO-N-suc-Fe(III) solution were measured in HBS at 37 ºC, at 60 MHz (1.41 T), using the five samples presented in Figure 28. Relaxivity studies presented a longitudinal ionic relaxivity (r_1) of 1.42 $mM^{-1}s^{-1}$ and a transversal relaxivity (r_2) of 1.62 $mM^{-1}s^{-1}$ for the DFO-N-suc-Fe(III)-liposomes. The low r_2/r_1 ratio (1:1) shows that the paramagnetic liposomes are best suited for positive contrast agent, T_1-weighted MRI. Both longitudinal and transversal relavixity of the liposomes was measured once.

The DFO-N-suc-Fe(III) complex showed a longitudinal relaxivity (r_1) of 1.42 mM^{-1}-s^{-1} and a transversal relaxivity (r_2) of 1.62 $mM^{-1}s^{-1}$.

In previous work in the present research group [25] the longitudinal (r_1) relaxivitiy of Fe-DFO was also measured presenting a r_1 of 1.3 $mM^{-1}s^{-1}$, at 1.41 T (pH = 5.4). The r_1 for Fe-DFO presented in the literature [55] measured at 20 MHz and 37 ºC is 1.4 mM-1s-1, which is around 3 times lower than the relaxivity of Gd-DTPA [56].

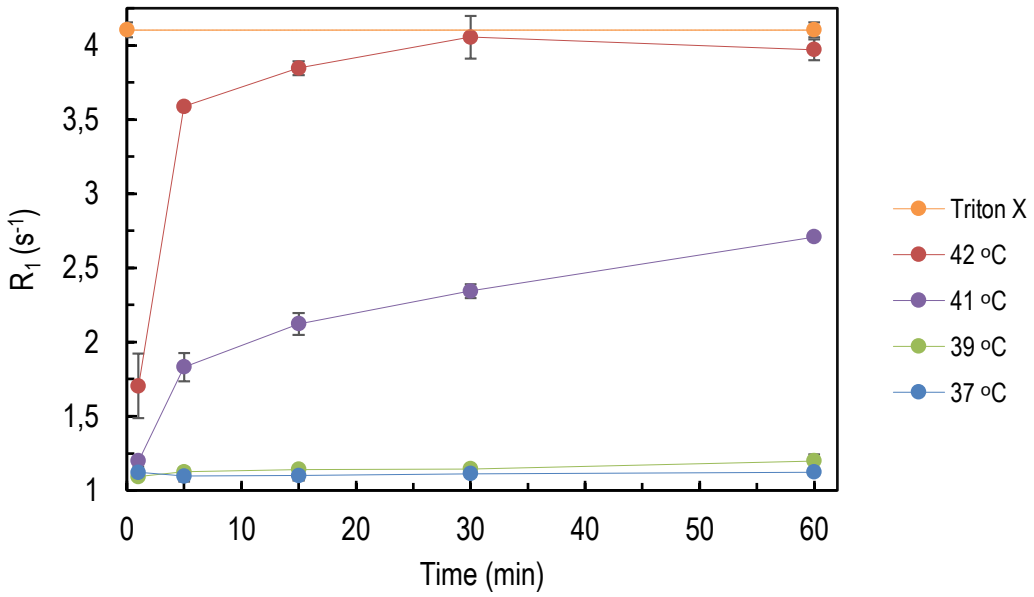

Figure 27. *Release of encapsulated DFO-N-suc-Fe(III) complex from the liposomal system measured at 1.41 T in 90 % FBS.*

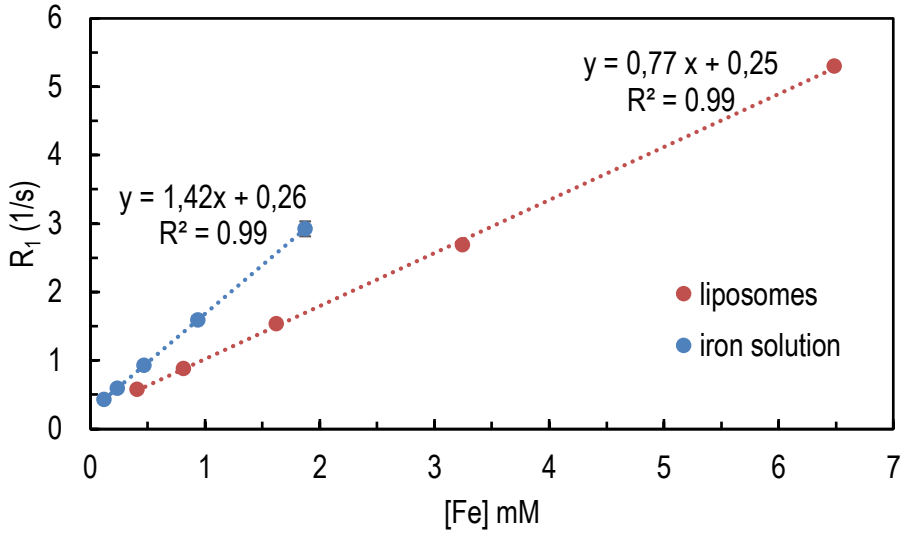

Figure 28. *R_1 vs [Fe] of DFO-N-suc-Fe(III) complex in HBS and of liposomes encapsulating DFO-N-suc-Fe(III) complex at 37 ºC measured at 1.41 T with the inversion recovery sequence. The slope of the graph shows the longitudinal relaxivity of 0.77 $mM^{-1}s^{-1}$. Inverse. Error bars indicate standard deviations.*

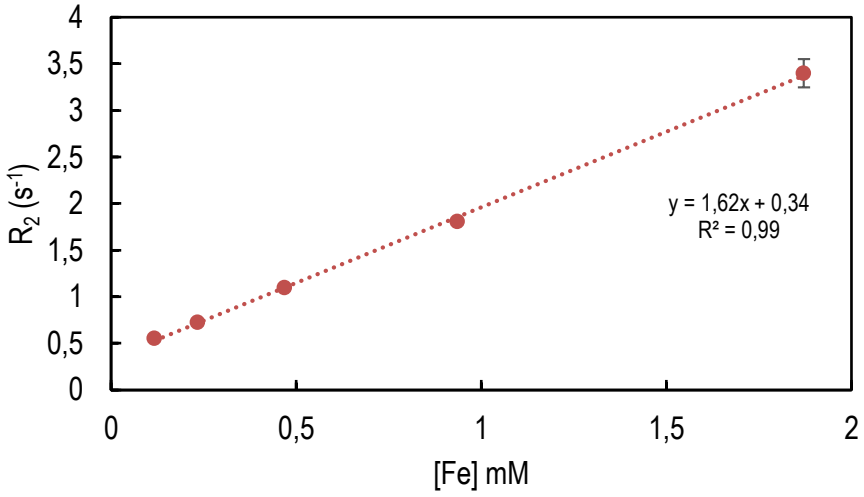

Figure 29. *Inverse T_2-relaxation times of liposomes. The T_2 was measured three times for each concentration sample point with the Carrr-Purcell-Meiboom-Gill. Error bars indicate standard deviations.*

4.3.2. Water exchange rate across the lipids bilayer

Measuring the T_1 relaxivity allows therefore to calculate the water permeability of the liposome membrane using a two-compartment model, where water molecules are distributed in the extra- and intraliposomal compartments, separated by the liposome membrane.

All the NMR measurements that were performed showed a significant increase in r_1 during heating at temperatures that are still below the phase transition temperature, T_m, due to the expected increase in water permeability of the lipid bilayer. As it can be seen by the heating cooling graphs, Figure 25 and Figure 26, the trans membrane water exchange rates at 37 ºC are higher compared to water exchange at 26 ºC In the experiment the water exchange rate was only measured at 37 ºC for TTSLs showing a k_{ex} of 285.45 s^{-1}.

4.3.3. Dynamic Light Scattering (DLS)

These liposomes encapsulating DFO-N-suc-Fe(III) complex yielded liposomes with a hydrodynamic radius of around 63 nm and a PD.I of 0.051, Figure 30, measured with dynamic light scattering.

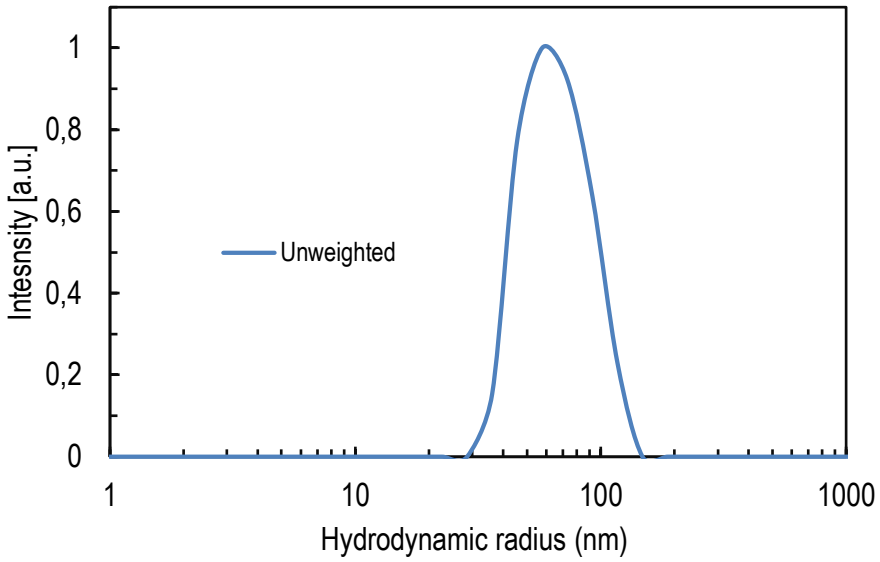

Figure 30. *Traditional temperature-sensitive liposomes were prepared encapsulating deferoxamine N-succimidyl Fe(III). These liposomes showed a hydrodynamic radius of around 63 nm and a PD.I of 0.051.*

4.3.4. Inductively Coupled Plasma (ICP)

The phosphorus (P) and iron (Fe) concentration were determined by means of inductive coupled plasma optical emission spectroscopy (ICP-OES).

Two samples were analyzed, one of deferoxamine N-succimidyl Fe(III) solution and another one of liposomes solution encapsulating deferoxamine N-succimidyl Fe(III). The concentration of iron in the deferoxamine N-succimidyl Fe(III) solution sample was 206 mM. In the sample of the liposomes solution the concentration of Fe was 32 mM and the concentration of phosphorus was 78 mM.

4.3.5. Cryo-Transmission Electron Microscopy

Cyro-TEM studies were performed to TTSLs (lipids: HSPC, DPPC, Cholesterol, DPPE-PEG2000) containing DFO-N-suc-Fe(III). The images were converted to a high quality JPEG format and are included below, Figure 31. Cryo-TEM showed liposomes with homogeneous sizes and a few multi-lamellar vesicles. More pictures can be seen in Appendix VI.

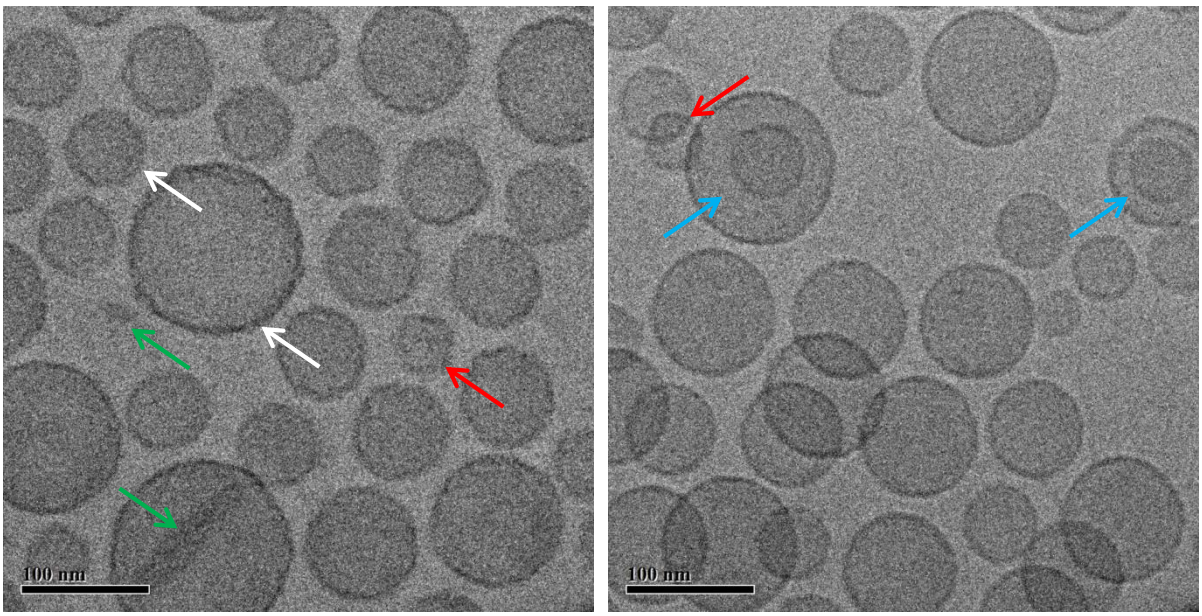

Figure 31. *Cryogen transmission electron microscopy (cryo-TEM) image of the DFO-N-suc-Fe(III) TTSLs. Large as well as small liposomes are visible. Most of the liposomes are spherical; some small liposomes are facetted and deformed (indicated by red arrows). Disc shaped micelles (indicated by green arrows) are visible in the upper left image. The blue arrows in the right image point at multi-lamellar vesicles. Some liposomes have irregular bilayers (indicated by white arrows). This may be inherent to the sample, but can also be caused by the electron beam.*

4.3.6. Differential Scanning Calorimetry

The melting phase transition temperature (T_m) of the liposome formulation was around 42 ºC, as evidenced from differential scanning calorimetry. A sharp phase transition was observed for TTSLs in, Figure 32, at 42.05 ºC with a standard deviation of 0.06.

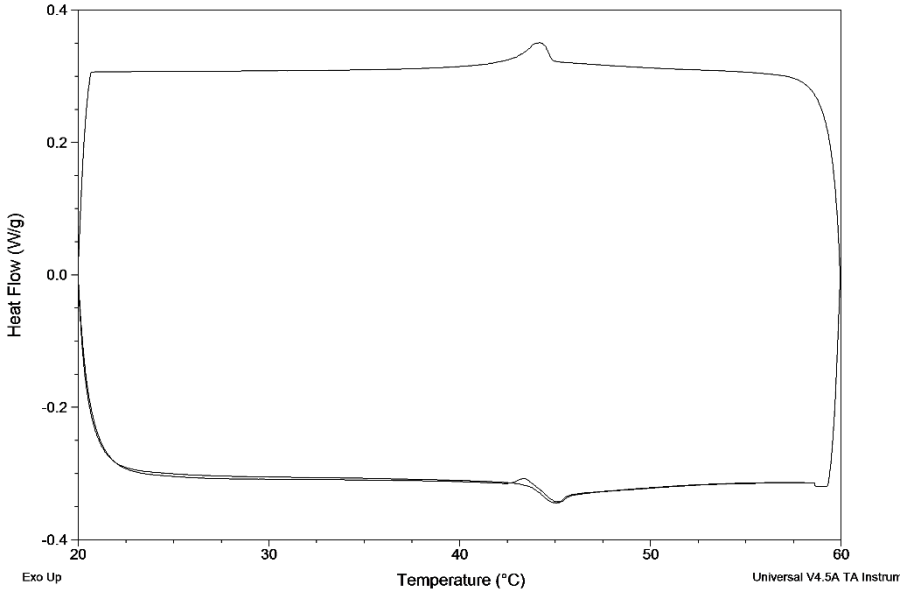

Figure 32. *DSC results of the TTSL formulation. A sharp phase transition was observed around 42 ºC.*

4.3.7. Magnetic Resonance Imaging

DFO-N-suc-Fe(III)-liposomes were diluted in HBS for further characterization *in vitro*. T_1 and T_2 relaxation times for all liposomal formulations, before and after heating to a temperature of T = 45 ºC for 30 minutes, were measured on a human 3 T MRI scanner. A T_1-weighted image, T_2-weighted image, T_1 map and T_2 map of heated and unheated samples of TTSLs encapsulating DFO-N-suc-Fe(III) complex with different concentrations gives the corresponding T_1 and T_2 values, Figure 33 and Table 2.

Before being heated for 30 minutes the four different concentrations of paramagnetic liposomes showed a lower T_1 value when compared to the T_1 value of the sample with a corresponding concentration after heating. This is due to the release of DFO-N-suc-Fe(III) complex. The same behavior is observed in the corresponding T_2 measurements however with a smaller change in T_2 when compared to the change in T_1 before and after heating. DFO-N-suc-Fe(III)-liposomes samples showed a decreasing positive contrast

with decreasing Fe^{3+} concentration (decreasing R_1 or increasing T_1). This experiment shows the potential for MR imaging when it is combined with this TSL in specific.

In Figure 34 the R_1 data are plotted against the corresponding DFO-N-suc-Fe(III) complex concentrations for the three most concentrated samples from Figure 33 before and after heating. The slope of a linear fit through these data points showed that the longitudinal relaxivity of 0.8 $mM^{-1}s^{-1}$ before heating and 1.2 $mM^{-1}s^{-1}$ after heating was obtained. For comparison, the relaxivity of free DFO-N-suc-Fe(III) complex in HBS was 0.77 $mM^{-1}s^{-1}$ at 1.41 T, Figure 28.

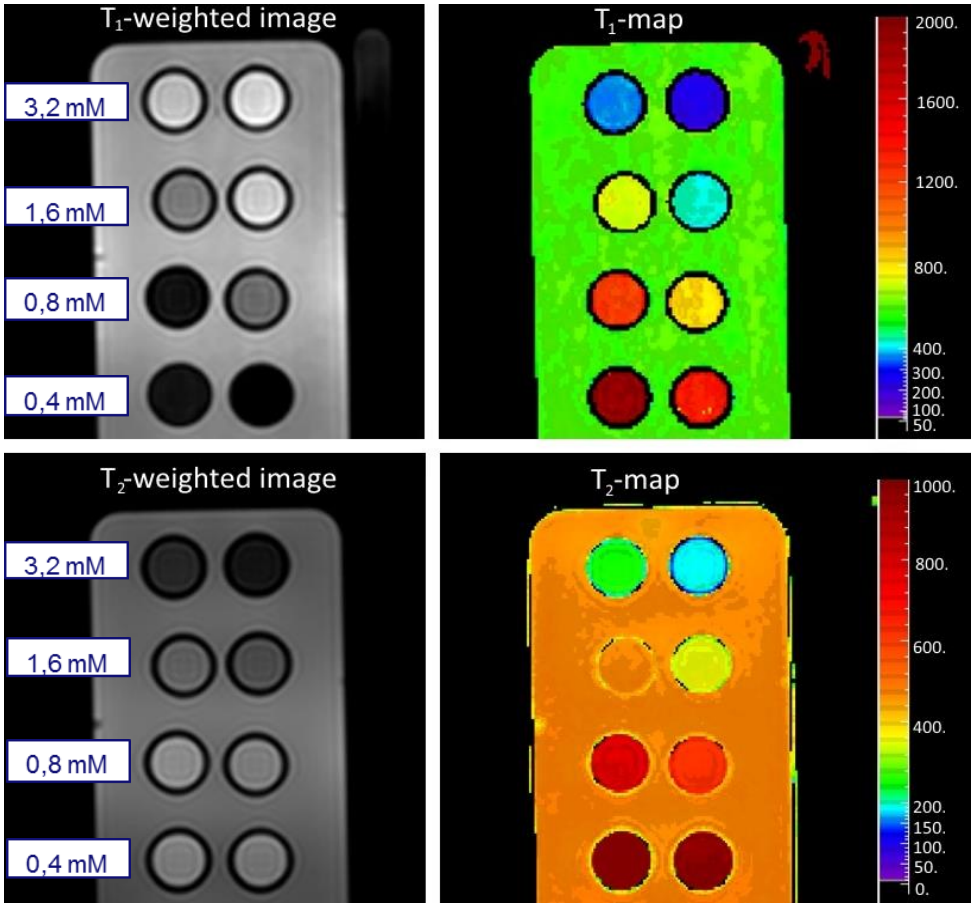

Figure 33. *T_1-weighted image (TI =1500 ms) (top left), T_1 map (top right), T_2-weighted picture (TE = 320 ms) (bottom left) and T_2 map (bottom right) before and after heating TTSLs with different DFO-N-suc-Fe(III) complex concentrations (3.2, 1.6, 0.8 and 0.4 mM). The sample holder contains a standard phantom solution (0.77 g/L CuSO4·5H2O and 2 g/L NaCl).*

Formulation	Concentration [Fe] (mM)	T_1 (ms) unheated	±	T_1 (ms) heated	±	T_2 (ms) unheated	±	T_2 (ms) heated	±
TTSL	3.2	363	8	234	9	251.01	1.38	186.41	1.63
	1.6	716	14	431	9	470.63	1.56	355.09	1.79
	0.8	1218	28	754	18	779.05	3.25	618.29	2.74
	0.4	1883	47	1196	46	1151.74	15.58	973.18	9.26

Table 2. *T_1 and T_2 values (± standard deviation) of TTSLs with different DFO-N-suc-Fe(III) complex concentrations (3.2, 1.6, 0.8 and 0.4 mM) before and after heating. The average and standard deviation were calculated from all the pixels within an ROI (region of interest) in the T_1 and T_2 maps.*

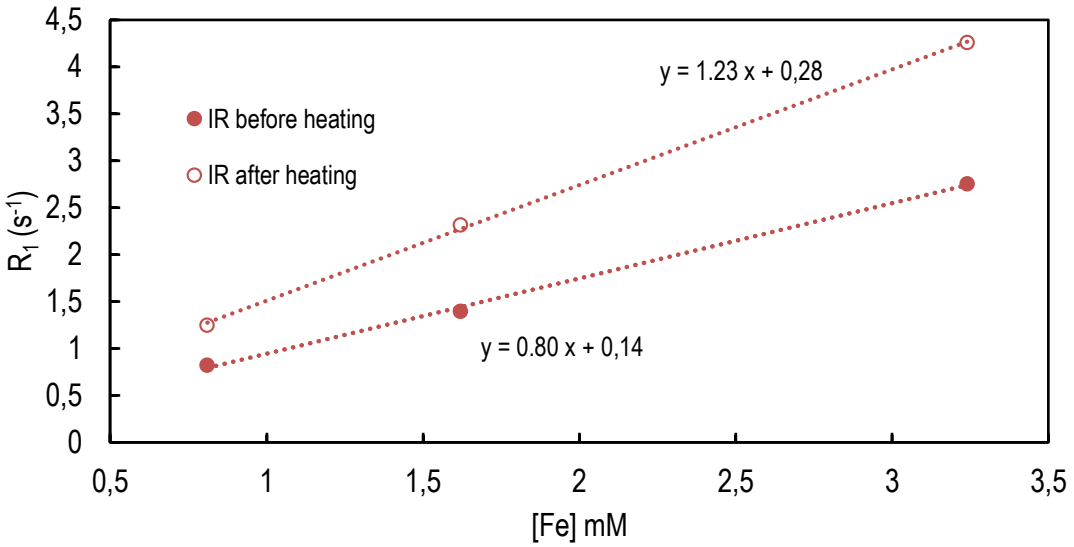

Figure 34. *R_1 vs [Fe] of DFO-N-suc-Fe(III) complex at 37 ºC measured at 3 T with the Look-Locker sequence and Inversion Recovery sequence. The slope of the graphs shows a relaxivity of 1.2 $mM^{-1}s^{-1}$ of released DFO-N-suc-Fe(III) complex and a relaxivity of 0.8 $mM^{-1}s^{-1}$ when the DFO-N-suc-Fe(III) complex is still encapsulated in the liposomes.*

4.3.8. HIFU mediated release in a gel phantom

As an *in vitro* experiment was performed for testing the MRI monitoring of HIFU-induced release of DFO-N-suc-Fe(III) complex from the TTSLs that were homogeneously distributed across the gel. After the HIFU application Look-Locker scans were performed for calculation of T_1 maps, Figure 35. The heated area showed a significant decrease of the T_1 value.

Before HIFU application left upper agarose spots showed a T_1 of 577 ms and the right upper agarose spot a T_1 of 590 ms. After HIFU application only the left spot was heated. Its T_1 value decreased to 427 ms which is consisted with the expected. The right spot was outside the area that was sonicated, however its T_1 value also decreased, from 590 ms to 478 ms. This could be due to the little distance between agarose spots or maybe a temperature gradient was developed from the heated area extending into the surrounding gel due to heat diffusion.

De Smet [38], showed that when MR-HIFU is used combined with temperature-sensitive liposomes (TSLs) co-encapsulating doxorubicin and 250 mM [Gd(HPDO3A)(H_2O)] a good correlation between the ΔR_1, the uptake of gadolinium and doxorubicin concentration in the tumor was achieved. Tumors that received local HIFU-mediated hyperthermia showed higher concentration of gadolinium and doxorubicin compared to the control group. When released from the liposomes, the DFO-N-suc-Fe(III) was 1.23 $mM^{-1}s^{-1}$. The r_1 of the [Gd(HPDO3A)(H2O)] contrast agent measured in the comparable experiment is 4.5 $mM^{-1}s^{-1}$ [45]. It can be concluded that to end with the same ΔR_1 and the same contrast three to four time more of DFO-N-suc-Fe(III) complex would be needed. In order to overcome this, an attempt could be made to encapsulate more ironin each liposome or to inject more liposomes since iron is not toxic as gadolinium.

Since the results of TTSLs encapsulating DFO-N-suc-Fe(III) are promising TTSLs encapsulating doxorubicin were also studied. The idea would be to co-inject both liposomes. The slow and incomplete release of doxorubicin from the TTSLs encapsulating only doxorubicin was not expected, as the same TTSL formulation containing both Dox and Gd shows a much faster and complete release [39]. Experiments regarding TTSLs encapsulating doxorubicin are in Appendix V.

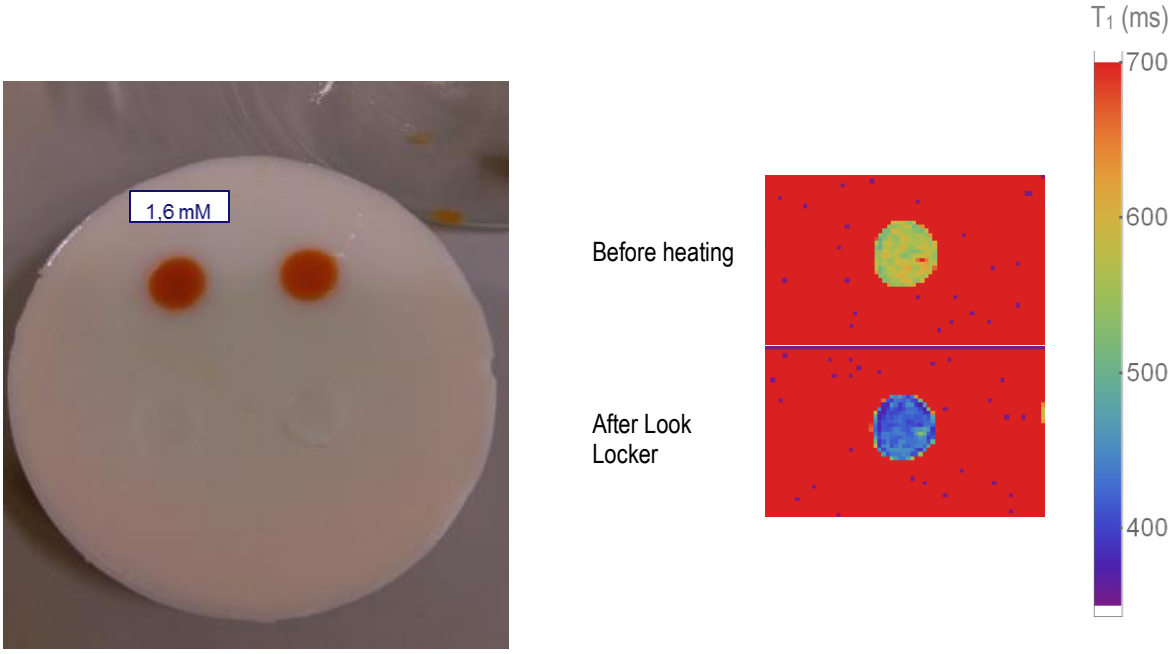

Figure 35. *Gel phantom (left), the two top orange spots contain TTSLs encapsulating DFO-N-suc-Fe(III) complex in a concentration of 1.6 mM and the bottom two spots are HBS to serve as a control; MR images (right) of a gel phantom containing TTSLs that encapsulate DFO-N-suc-Fe(III) complex. T_1 maps before and after hyperthermia with a sonication diameter of 4 mm.*

5. General Discussion and Conclusions

Gadolinium (Gd) and Manganese (Mn)-based CAs have been used to monitor doxorubicin release. Both of these MRI contrast agents pose potential health risks and therefore TSLs-based image-guided drug delivery has so far been limited to preclinical research. The use of TSLs co-encapsulating doxorubicin and [Gd(HPDO3A)(H_2O)] under MR image guidance for HIFU-mediated drug delivery has the potential to assess the efficacy of the drug delivery to the tumor. As long as Gd-based MR CAs (including ([Gd(HPDO3A)(H_2O)])) are chelated they are quickly cleared by the kidney. Nevertheless patients that suffered from severe renal impairment have developed nephrogenic systemic fibrosis (NSF).

Trying to overcome the limitations above mentioned the research group moved to a different approach, an alternative MR-imageable liposome. However, the contrast agent Fe^{3+}-deferoxamine (Fe-DFO) release characteristics were inferior with respect to its Gd loaded counterpart. The release of the contrast agent was expected to happen quickly at a specific melting phase temperature, T_m, however, for Fe-DFO the release happened gradually.

In this study TSLs encapsulating Fe-based contrast agents were studied in great detail. The release kinetics and stability were investigated. A novelty of the synthesized nanoparticles in this study is that the liposomes encapsulate DFO-N-suc-Fe(III) complex as a MR contrast agent, a Fe-DFO derivate. This nanoparticle yields a lower T_1-contrast with respect to Gd^{3+}-particles, but does not have the intrinsic problem of potential Gd^{3+}-toxicity, which precluded clinical translation of Gd-based nanoparticles in the past [46].

The net Fe^{3+} load of a liposome injection represents only a minor fraction compared to the Fe^{3+} concentration naturally present in blood and tissues. Toxicity or adverse effects are not expected from DFO-N-suc-Fe(III) complex uptake in liver and spleen in contrast to Gd-based nanoparticles that pose a threat to induce nephrogenic systemic fibrosis (NSF).

Measurements of the longitudinal relaxation rate R_1 as a function of temperature indicate that DFO-N-suc-Fe(III) complex (from TTSLs) is released at a T_m between 41 ºC and 42 ºC in contrast with Fe-DFO that is only released at higher temperatures (between 42 ºC and 45 ºC). Moreover, the release of DFO-N-suc-Fe(III) is fast while the release of Fe-DFO seemed to occur more gradually. Measurements at constant temperatures revealed a steady release of DFO-N-suc-Fe(III) complex within the first 15 minutes, which could be improved by tuning the lipid formulation. These liposomes were very stable at body temperature and even at 39 ºC, which was a large improvement compared to TTSLs encapsulating Fe-DFO.

The aim of this research was to improve the liposomal release of the CA as well as the stability of the liposomal formulation. Both improvements in release and stability were achieved by adapting the Fe-DFO complex used, which allowed a higher intraliposomal pH, thereby minimizing the risk of hydrolysis. The association of Fe-DFO with doxorubicin was avoided by opting for a co-injection instead of co-encapsulation.

The next steps include some slight adaptations to the lipid formulation, attempting to load more of the complex into the liposome. Once the formulation is completely fine-tuned, a suitable doxorubicin-loaded formulation should be found. The final step would be to inject *in vivo* and to see if chemodosimetry for TSLs using Fe-based liposomal contrast agents is possible.

This class of contrast agent creates opportunities for monitoring drug release with MRI in response to local hyperthermia avoiding the drawbacks of Gd-based contrast agents.

6. References

1. Trinkaus KM, Miller JP, Papageorgio C, et al. The Washington Manual of Oncology. 1st ed. Williams and Wilkins; 2002.

2. Bonadonna G, D SMM, Lena MDE, Fossati-bellani F. Clinical Evaluation of Adriamycin , a New Antitumour Antibiotic. British Medical Journal. 1969;3:503-6.

3. Lown JW. Discovery and development of anthracycline antitumour antibiotics. Chemical Society Reviews. 1993;22(3):165-76.

4. Licata S, Saponiero A, Mordente A, Minotti G. Doxorubicin Metabolism and Toxicity in Human Myocardium: Role of Cytoplasmic Deglycosidation and Carbonyl Reduction. Chem Res Toxicol. 2000;13(5):414-420.

5. Langereis S, Hijnen N, Strijkers G, Nicolay K, Grull H. Multifunctional liposomes for MRI and image-guided drug delivery. Ther Deliv. 2014;5(1):21-24.

6. Souto, EB. Lipid Nanocarriers in Cancer Diagnosis and Therapy. 1st ed. Smithers Rapra Technology; 2011

7. Allen TM, Cullis PR. Drug Delivery Systems : Entering the Mainstream. Science. 2004; 303:1818-22.

8. Torchilin VP. Targeted pharmaceutical nanocarriers for cancer therapy and imaging. AAPS J. 2007;9(2):E128-E147.

9. Abraham SA, Waterhouse DN, Mayer LD, Cullis PR, Madden TD, Bally MB. The liposomal formulation of doxorubicin. Methods Enzymol. 2005;391:71-97.

10. Matsumura Y, H. Maeda. A new concept for macromolecular therapeutics in cancer chemotherapy: mechanism of tumoritropic accumulation of proteins and the antitumor agent smancs. Cancer Res. 1986;46:6387-92.

11. Drummond DC, Meyer O, Hong KL, et al. Optimizing liposomes for delivery of chemotherapeutic agents to solid tumors. Pharmacological Reviews. 1999;51(4):691-743.

12. Grull H, Langereis S. Hyperthermia-triggered drug delivery from temperature-sensitive liposomes using MRI-guided high intensity focused ultrasound. J Control Release. 2012;161(2):317-27.

13. Weinstein JN, Magin RL, Yatvin MB, et al. Liposomes and local hyperthermia- selective delivery of methotrexate to heated tumors. Science. 1979;204(4389):188-91.

14. Yatvin MB, Weinstein JN, Dennis WH, et al. Design of liposomes for enhanced local release of drugs by hyperthermia. Science. 1978;202:1290-3.

15. Hong C, Libutti S, Wood B. Liposomal doxorubicin plus radiofrequency ablation for complete necrosis of a hepatocellular carcinoma. Curr. Oncol. 2013;20:274-277.

16. Mabrey S, Sturtevant JM. Investigation of phase transitions of lipids and lipid mixtures by sensitivity differential scanning calorimetry. Proc Natl Acad Sci U S A. 1976;73(11):3862-3866.

17. Needham D, Anyarambhatla G, Kong G. A New Temperature-sensitive Liposome for Use with Mild Hyperthermia : Characterization and Testing in a Human Tumor Xenograft Model Advances in Brief A New Temperature-sensitive Liposome for Use with Mild Hyperthermia : Characterization and Testing in a H. 2000:1197-1201.

18. Oja CD, Semple SC, Chonn A, Cullis PR. Influence of dose on liposome clearance: Critical role of blood proteins. Biochim Biophys Acta - Biomembr. 1996;1281(1):31-37.

19. Immordino ML, Dosio F, Cattel L. Stealth liposomes: Review of the basic science, rationale, and clinical applications, existing and potential. Int J Nanomedicine. 2006;1(3):297-315.

20. Maeda H. Tumor-Selective Delivery of Macromolecular Drugs via the EPR Effect: Background and Future Prospects. Bioconjugate Chemistry. 2010;21(5):797-802.

21. Hofheinz R-D, Gnad-Vogt SU, Beyer U, Hochhaus A. Liposomal encapsulated anti-cancer drugs. Anticancer Drugs. 2005;16(7):691-707.

22. Kong G, Anyarambhatla G, Petros WP, et al. Efficacy of liposomes and hyperthermia in a human tumor xenograft model: importance of triggered drug release. Cancer Res. 2000;60:6950-7.

23. Landon CD, Park J, Needham D, et al. Nanoscale drug delivery and hyperthermia: The materials design and preclinical and clinical testing of low temperature-sensitive liposomes used in combination with mild hyperthermia in the treatment of local cancer. The Open Nanomedicine Journal. 2011;3:38-64.

24. Gasselhuber A, Dreher MR, Negussie A, Bradford J, Rattay F, Haemmerich D. NIH Public Access. 2010;26(5):499-513.

25. Lindner LH, Eichhorn ME, Eibl H, et al. Novel Temperature-Sensitive Liposomes with Prolonged Circulation Time. Clin Cancer Res. 2004;10:2168-2178.

26. Hossann M, Wiggenhorn M, Schwerdt A, et al. In vitro stability and content release properties of phosphatidylglyceroglycerol containing thermosensitive liposomes. Biochim Biophys Acta. 2007;1768(10):2491-2499.

27. Hossann M, Wang T, Syunyaeva Z, et al. Non-ionic Gd-based MRI contrast agents are optimal for encapsulation into phosphatidyldiglycerol-based thermosensitive liposomes. J Control Release. 2013;166(1):22-29.

28. Fossheim SL, Fahlvik AK, Klaveness J, Muller RN. Paramagnetic liposomes as MRI contrast agents: Influence of liposomal physicochemical properties on the in vitro relaxivity. Magn Reson Imaging. 1999;17(1):83-89.

29. Mulder WJM, Strijkers GJ, van Tilborg G a F, Griffioen AW, Nicolay K. Lipid-based nanoparticles for contrast-enhanced MRI and molecular imaging. NMR Biomed. 2006;19(1):142-164.

30. Bushberg J, Boone J. The essential physics of medical imaging. 2nd ed. Williams and Wilkins; 2002.

31. Reichenbach JR, Hackländer T, Harth T, Hofer M, Rassek M, Mödder U. 1H T1 and T2 measurements of the MR imaging contrast agents Gd-DTPA and Gd-DTPA BMA at 1.5T. Eur Radiol. 1997;7(2):264-274.

32. Estelrich J, Sánzhez-Martín MJ, Busquets MA. Nanoparticles in magnetic resonance imaging : from simple to dual contrast agents. Press D. 2015:1727-1741.

33. Vaupel P, Mayer A. Hypoxia in cancer: significance and impact on clinical outcome. Cancer Metastasis Rev. 2007;26(2):225-239.

34. Fossheim SL, K.A. Il'yasov, J. Hennig, A. Bjørnerud. Thermosensitive paramagnetic liposomes for temperature control during MR Imaging-guided hyperthermia: In vitro feasibility studies. Acad Radiol. 2000;7(12):1107-15.

35. Ponce AM, Viglianti BL, Yu D, et al. Magnetic resonance imaging of temperature-sensitive liposome release: drug dose painting and antitumor effects. J Natl Cancer Inst. 2007;99(1):53-63.

36. Viglianti BL, Ponce AM, Michelich CR, et al. Chemodosimetry of in vivo tumor liposomal drug concentration using MRI. Magn Reson Med. 2006;56(5):1011-1018.

37. Negussie AH, Yarmolenko PS, Partanen A, et al. Formulation and characterisation of magnetic resonance imageable thermally sensitive liposomes for use with magnetic resonance-guided high intensity focused ultrasound. International Journal of Hyperthermia. 2011;27(2):140-55.

38. De Smet M, Heijman E, Langereis S, Hijnen NM, Grüll H. Magnetic resonance imaging of high intensity focused ultrasound mediated drug delivery from temperature-sensitive liposomes: an in vivo proof-of-concept study. J Control Release. 2011;150(1):102-110.

39. De Smet M, Langereis S, van den Bosch S, Grüll H. Temperature-sensitive liposomes for doxorubicin delivery under MRI guidance. J. Control. Release 2010;143(1):120-7.

40. Guzman ML, Rossi RM, Karnischky L, et al. The sesquiterpene lactone parthenolide induces apoptosis of human acute myelogenous leukemia stem and progenitor cells. Blood. 2005;105(11):4163-4169.

41. Tempany CMC, McDannold NJ. Focused ultrasound surgery in oncology: overview and principles. Radiology. 2011;259(1):39-56.

42. Hijnen NM. Preclinical Evaluation of MR-HIFU Based Thermal Cancer Therapies. PhD Thesis. 2013. Eindhoven: Technische Universiteit Eindhoven.

43. Langereis S, Geelen T, Grüll H, Strijkers GJ, Nicolay K. Paramagnetic liposomes for molecular MRI and MRI-guided drug delivery. *NMR Biomed*. 2013;26(7):728-744.

44. Hahn GM, Braun J, Har-kedartf I. Thermochemotherapy: Synergism Between Hyperthermia (42-43º) and Adriamycin (or Bleomycin) in Mammalia Cell Inactivation. Proc Natl Acad Sci USA. 1975;72(3):937-940.

45. Smet M. MR-HIFU Mediated Local Drug Delivery Using Temperature-Sensitive Liposomes, PhD Thesis. 2013. Eindhoven: Technische Universiteit Eindhoven.

46. Weinreb JC, Abu-Alfa AK. Gadolinium-based contrast agents and nephrogenic systemic fibrosis: why did it happen and what have we learned? *J Magn Reson Imaging*. 2009;30(6):1236-1239.

47. Hijnen N, Elevelt A, Grüll H. Stability and Trapping of Magnetic Resonance Imaging Contrast Agents During High-Intensity Focused Ultrasound Ablation Therapy. *Invest Radiol*. 2013;48(7).

48. Hummelink M, Novel Fe-based nanoparticles contrast agents for T1-weighted MR imaging purposes. MSc Thesis. 2014. Eindhoven: Technische Universiteit Eindhoven.

49. Hou X, Jones BT. Inductively Coupled Plasma / Optical Emission Spectrometry (Encyclopedia of Analytical Chemistry). 2008.

50. Boss CB, Fredeen KJ. Concepts, Instrumentation and Techniques in Inductively Coupled Plasma Optical Emission Spectroscopy. 3rd ed. Perkin Elmer; 2004.

51. Motion B. Dynamic Light Scattering : An Introduction in 30 Minutes. DLS technical note MRK656-01, Malvern Instruments.

52. ALV-Technical Documentation (ALV(CGS-3 Compact Goniometer System). 2014.

53. Gill P, Moghadam TT, Ranjbar B. Differential scanning calorimetry techniques: applications in biology and nanoscience. J Biomol Tech. 2010;21(4):167-193.

54. Liu ZD, Hider RC. Design of iron chelators with therapeutic application. Coord Chem Rev. 2002;232(1-2):151-171.

55. Duewell S, Wüthrich R, Von Schulthess GK, Jenny HB, Muller RN, Moerker T, Fuchs, WF. Nonionic Polyethylene Glycol-Ferrioxamine as a Renal Magnetic Resonance Contrast Agent. Invest Radiol. 1991;26:50-57.

56. Rohrer M, Bauer H, Mintorovitch J. Comparison of Magnetic Properties of MRI Contrast Media Solutions at Different Magnetic Field Strengths. Investigative Radiology. 2005;40(11):715-724.

57. http://www.avantilipid.com (May 2015) .

7. Appendix

Appendix I – Clinical MR-HIFU System

In Figure 36 a schematic representation of temperature-induced drug delivery using the MR-HIFU system can be seen.

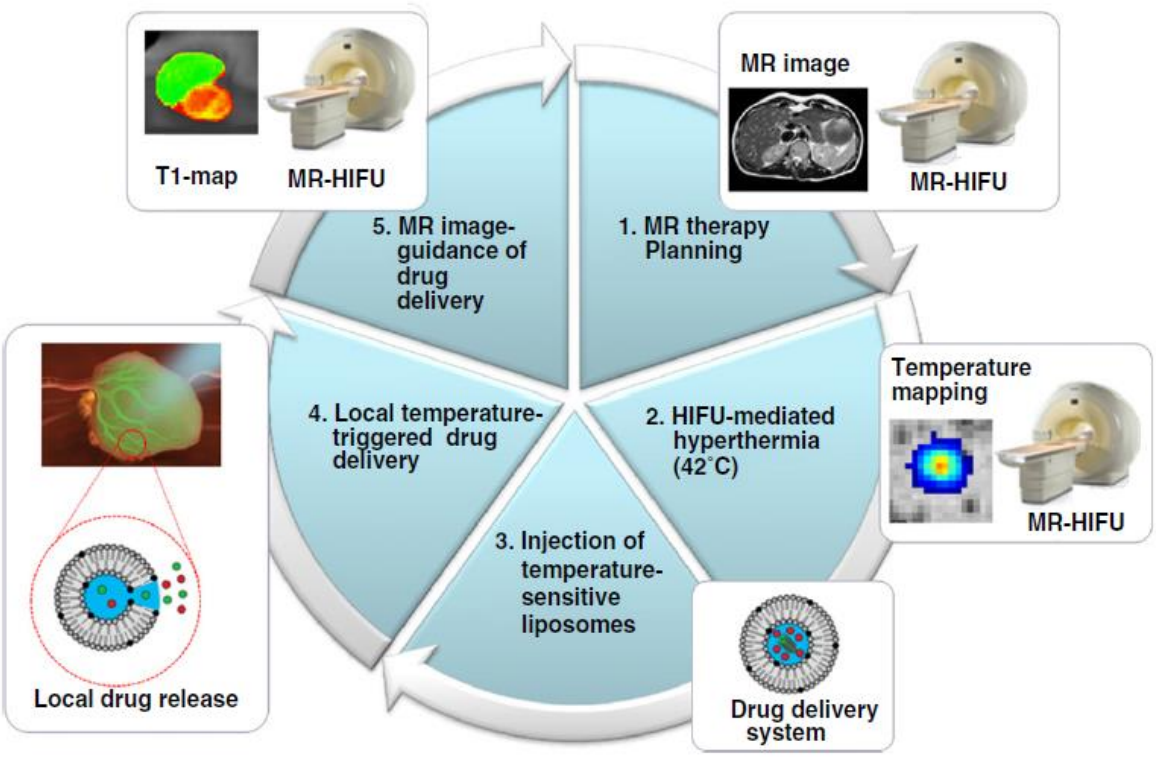

Figure 36. *Schematic representation of temperature-induced drug delivery using MR-HIFU and temperature-sensitive liposomes that encapsulate drug and MRI CAs. MRI plays a role in planning adequate treatment, during treatment for providing feedback regarding temperature as well as in evaluating the treatment* [12]***.***

Appendix II – Chemical Structure of Materials

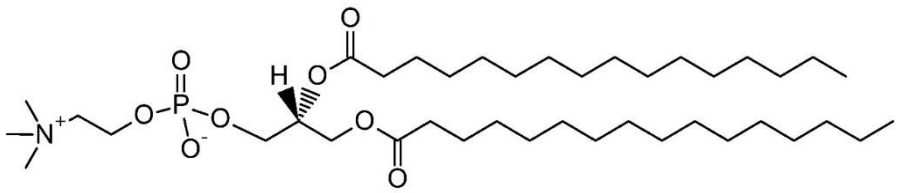

Figure 37. *DPPC, chemical formula: $C_{40}H_{80}NO_8P$; molecular weight (MW): 734.04 g/mol.*

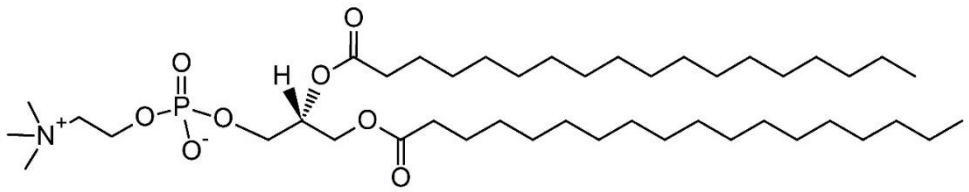

Figure 38. *DSCP, chemical formula: $C_{44}H_{88}NO_8P$; MW: 790.15 g/mol.*

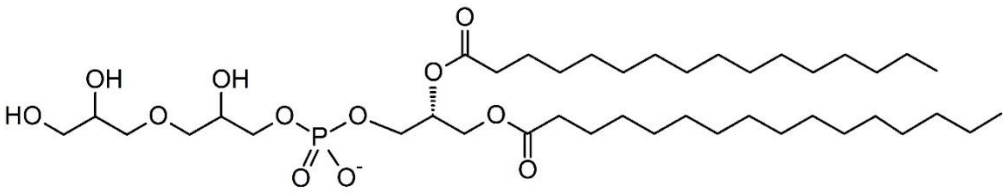

Figure 39. *DPPGOG, chemical formula: $C_{41}H_{80}O_{12}P$; MW: 819.04 g/mol.*

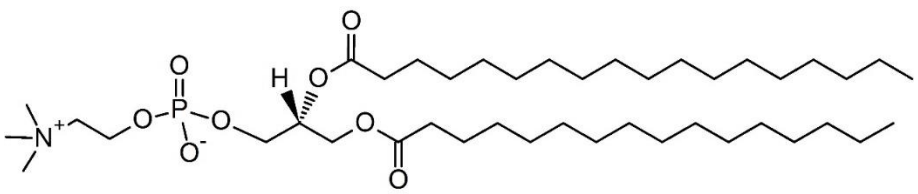

Figure 40. *HSPC, chemical formula $C_{42}H_{84}NO_8P$; MW: 762.09 g/mol.*

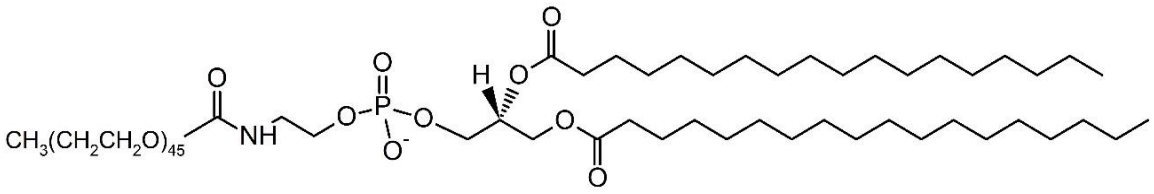

Figure 41. *DPPE-PEG2000, chemical formula: $C_{129}H_{259}N_2O_{55}P$; MW: 2749.43 g/mol.*

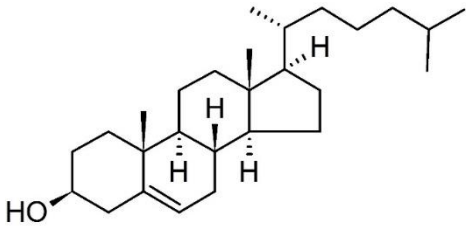

Figure 42. *Cholesterol, chemical formula: $C_{27}H_{46}O$; MW: 286.65 g/mol.*

Appendix III – Synthesis of Liposomes

Properties of lipid formulations can vary depending on the composition, however, the same preparation method can be used for all lipid vesicles regardless of composition. The general elements of the procedure involve preparation of the lipid for hydration, hydration with agitation, and sizing to a homogeneous distribution of vesicles.

Creating a Lipid Film

The liposomes were made by the lipid-film hydration technique. Phospholipids and cholesterol (it is added in order to improve stability) were dissolved in chloroform/methanol (7:3 v/v) to retrieve a homogeneous solution, Figure 43. The solvent was then removed by rotary evaporation under vacuum, at 55 ºC, yielding a thin lipid film (350-200 mbar in steps during 10 minutes, 200 mbar for 15 minutes, making sure the lipid film is already looking dry, 0 mbar for one hour). The lipid film was kept under nitrogen flow overnight to remove traces of solvent.

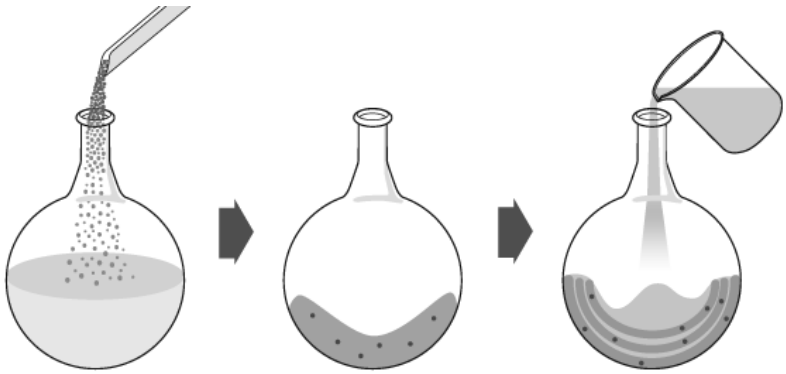

Figure 43. *Lipid film making. The phospholipids and the cholesterol are dissolved in chloroform/methanol (in the left); thin lipid film after being dried under nitrogen (in the middle); hydration of the lipid film (in the right), adapted from* [57]*.*

Hydration

The previous lipid film was hydrated, at 60 ºC by adding a mixture of glass marbles, buffer containing a contrast agent or not, in a phospholipid concentration between 50 mM and 70 mM. Large multilamellar

vesicles (LMVs) were obtained by doing this for at for at least 30 minutes, Figure 44 (left and middle figures).

Extrusion

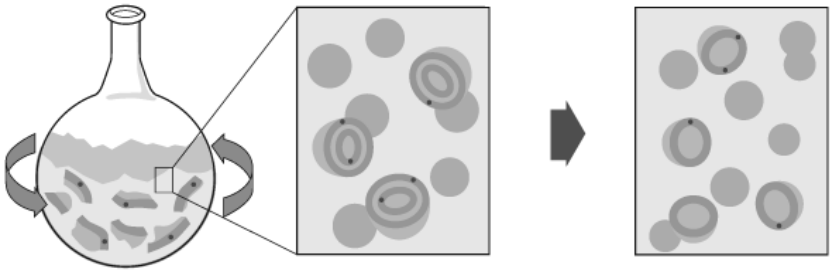

Figure 44. *Hydration (in the left)**;** large multilamellar vesicles (in the middle), before extrusion process; small unilamellar vesicles (in the right) after extrusion process, adapted from* [57].

Lipid extrusion is a technique in which a lipid suspension is forced through a polycarbonate filter with a defined pore size to yield particles having a diameter near the pore size of the filter used. The hydrated LMV suspensions were downsized 1 time through a 200 nm 2 times through a double 200 nm filter and 6 times through a 100 nm polycarbonate filter, at 60 ºC, using a Lipex 10 mL extruder.

Washing and Concentration

After extrusion, the extraliposomal buffer was replaced by HEPES buffered saline (HBS), pH=7.8 by gel filtration through a PD-10 column (GE Healthcare).

Note*: When temperature-sensitive liposomes were encapsulated with doxorubicin (and not with the contrast agent) there was an additional step following the previous one; the temperature-sensitive liposomes were loaded with doxorubicin. After the solution was passed through a PD-10 column to remove traces of unencapsulated doxorubicin.*

Subsequently, the liposomes were washed (using Amicon Ultra-15 centrifual filter unit or PD-10 columns) with HEPES buffered saline (HBS), pH 7.8 and concentrated using Amicon Ultra-15 centrifugal filter unit (100 kDa MWCO, Molecular Weight Cutoff, Milipore, UK) at 4000xG in an Heraeus Biofuge (Thermo Scientific, US).

Doxorubicin Loaded DPPGOG-TSLs

A total amount of 300 µmol of phospholipids (DPPC:DSPC:DPPGOG = 50:20:30) were dissolved in chloroform/methanol (7:3 v/v) solution in a 500 mL round bottom flask. The organic solvents were removed *in vacuo* until a thin lipid film was formed, which was further dried overnight under a nitrogen flow. Multilamellar vesicles were created by hydrating the lipid film with a 300 mM citrate buffer (pH 4) in a phospholipid concentration of 50 mM. The suspension was extruded successively at 60 ºC. After extrusion, the extraliposomal buffer was replaced by HEPES Buffered Saline (HBS), pH 7.8 (20 mM HEPES and 137 mM NaCl) by gel filtration through a PD-10 column. The doxorubicin solution in saline (2mg/mL) was added to the liposomes at a 20:1 phospholipid to doxorubicin weight ratio and incubated at 37 ºC for 60 minutes. Finally, the liposomes were passed through another PD-10 column to remove traces of unencapsulated doxorubicin. Amicon Ultra-15 spin filter devices were used to concentrate the liposomes.

Regarding doxorubicin loading a commonly used procedure to prepare liposomes with a transmembrane pH gradient relies on the entrapment of a 300 mM citrate buffer, pH 4.0. Citrate is a triprotic buffer and possesses a large buffering capacity in the range of pH 3–6.5. The drug should be encapsulated in the liposomes by remote-loading, exploiting the pH gradient that was created by changing the outer buffer to HBS, pH 7.8.

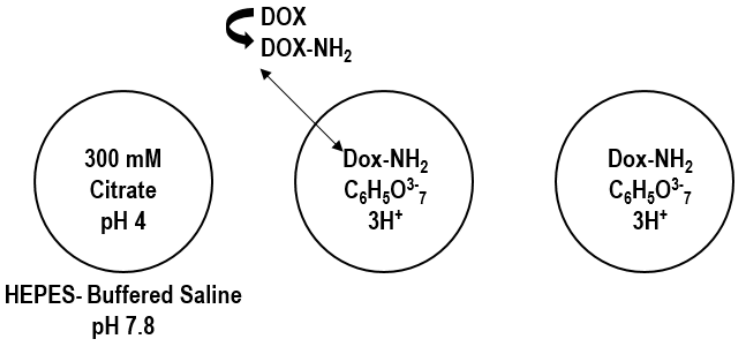

Figure 45. *Citrate loading procedure. Method to encapsulate doxorubicin into liposomes. Here the liposomes are prepared in 300 mM citrate buffer, pH 3.5, and the extraliposomal buffer is replaced by HEPES-buffered saline at pH 7.5, adapted from* [9]*.*

Deferoxamine Fe(III) Loaded DPPGOG-TSLs

Deferoxamine Fe(III) loaded DPPGOG-TSLs were prepared in two different ways using two different intraliposomal buffers: HBS (20 mM HEPES and 137 mM NaCl, pH 7.8) and acetate buffer (0.2 M sodium acetate and 0.2 M acetic acid, pH 4).

A total amount of 150 µmol of phospholipids (DPPC:DSPC:DPPGOG = 50:20:30) were dissolved in chloroform/methanol. The organic solvents were removed *in vacuo* until a thin lipid film was formed, which was further dried overnight under a nitrogen flow.

Using HBS as a buffer: 750 µmol of deferoxamine mesylate and $FeCl_3.6H_2O$ were dissolved in HBS and mixed under mechanical stirring (pH < 1), resulting in Fe^{3+}-Deferoxamine (Fe-DFO). NaOH was used to increase the pH above 5.

Using acetate as a buffer: 750 µmol of deferoxamine mesylate and 2 % less of $FeCl_3.6H_2O$ were dissolved in MilliQ separately. The pH of the deferoxamine solution (around 4.5) was lowered with HCL (2 M) to pH 3. Drops of $FeCl_3.6H_2O$ dissolved in MilliQ were added to the deferoxamine solution and mixed under mechanical stirring, resulting in Fe^{3+}-Deferoxamine (Fe-DFO), with pH <1. 10 mM of acetate and NaOH were used to buffer and to increase the pH to 4.

Then the Fe-DFO solution was filtered over a 0.22 µm syringe filter in order to remove non-complexated iron. The obtained lipid film was hydrated, at 60 ºC, with 240 mM of Fe-DFO solution in a phospholipid concentration of 50 mM. The suspension was extruded successively at 60 ºC.

After extrusion, the encapsulated liposomes were washed with HBS in Amicon Ultra centrifugal filters (50k MWCO) (Milipore, UK) at 4000xG in a Heraeus Biofuge (Thermo Scientific, US). Subsequently, the extraliposomal buffer was replaced by HEPES buffered saline (HBS), pH 7.8 by gel filtration through a PD-10 column (GE Healthcare) and the liposomes were washed again until no unencapsulated Fe-DFO was present.

Deferoxamine-N-succimidyl Fe(III) Loaded DPPGOG-TSLs

Deferoxamine-N-succimidyl Fe(III) loaded DPPGOG-TSLs were prepared in two different ways using two different intraliposomal buffers: Tris powder (40 mM, pH 8), whose pH is temperature dependent and Gly-Gly (40 mM, pH 8.5).

A total amount of 210 µmol of phospholipids (DPPC:DSPC:DPPGOG = 50:20:30) were dissolved in chloroform/methanol. The organic solvents were removed *in vacuo* until a thin lipid film was formed, which was further dried overnight under a nitrogen flow.

Using Trizma as a buffer: 300 µmol of deferoxamine-N-succimidyl Fe(III) were dissolved in MilliQ resulting in a solution with pH 3. The pH was raised to 8.5 with NaOH and 40 mM of Trizma buffer were added to buffer the solution. Then the solution was filtered over a 0.22 µm syringe filter in order to remove non-complexated iron. The obtained lipid film was hydrated, at 60 ºC, with 85 mM of iron solution in a phospholipid concentration of 70 mM. The suspension was extruded successively at 60 ºC.

Using Gly-Gly as a buffer: 750 µmol of deferoxamine-N-succimidyl Fe(III) were dissolved in MilliQ resulting in a solution with pH 3. The pH was raised to 8.5 with NaOH and 40 mM of Gly-Gly buffer were added to buffer the solution. Then the solution was filtered over a 0.22 µm syringe filter in order to remove non-complexated iron. The obtained lipid film was hydrated, at 60 ºC, with 210 mM of iron solution in a phospholipid concentration of 70 mM. The suspension was extruded successively at 60 ºC.

After extrusion, the liposomes were washed and concentrated like in the previous liposome experiments.

Deferoxamine-N-succimidyl Fe(III) Loaded TTSLs

Deferoxamine N-succimidyl Fe(III) loaded TTSLs were using Gly-Gly (40 mM, pH 8.5) as intraliposomal buffer.

A total amount of 204 µmol of phospholipids (DPPC:HSPC:Chol:DPPE-PEG2000 = 50:25:15:3) were dissolved in chloroform/methanol. The organic solvents were removed *in vacuo* until a thin lipid film was formed, which was further dried overnight under a nitrogen flow.

Using Gly-Gly as a buffer: 1020 µmol of deferoxamine-N-succimidyl Fe(III) were dissolved in MilliQ resulting in a solution with pH 3. The pH was raised to 8.5 with NaOH and 40 mM of Trizma buffer were added to buffer the solution. Then the solution was filtered over a 0.22 µm syringe filter in order to remove non-complexated iron. The obtained lipid film was hydrated, at 60 ºC, with 220 mM of iron solution in a phospholipid concentration of 50 mM. The suspension was extruded successively at 60 ºC.

After extrusion, the encapsulated liposomes were washed and concentrated.

Doxorubicin Loaded TTSLs

A total amount of 250 μmol of phospholipids (DPPC:HSPC:Chol:DPPE-PEG2000 = 50:25:15:3) were dissolved in chloroform/methanol (7:3 v/v) solution in a 500 mL round bottom flask. The organic solvents were removed *in vacuo* until a thin lipid film was formed, which was further dried overnight under a nitrogen flow. Multilamellar vesicles were created by hydrating the lipid film with a 240 mM ammonium buffer, $(NH_4)2SO_4$ (pH 5.5) in a phospholipid concentration of 50 mM. The suspension was extruded successively at 60 ºC. After extrusion, the extraliposomal buffer was replaced by HEPES Buffered Saline (HBS), pH 7.8 (20 mM HEPES and 137 mM NaCl) by gel filtration through a PD-10 column. The doxorubicin solution in HBS (5 mg/mL) was added to the liposomes at a 20:1 phospholipid to doxorubicin weight ratio and incubated at 37 ºC for 60 minutes. Finally, the liposomes were passed through another PD-10 column to remove traces of unencapsulated doxorubicin. Amicon Ultra-15 spin filter devices were used to concentrate the liposomes. After extrusion, the encapsulated liposomes were washed and concentrated [39].

Appendix IV – Gel Phantoms for HIFU Experiments

Aim: Prepare a phantom for MRI (Magnetic Resonance Imaging) to investigate how DFO-N-suc-Fe(III) complex that were originally encapsulated in TTSLs diffuses over the gel phantom when HIFU is applied.

Method:

A: Preparation of the bigger gel

2 % agar + 2 % silica (w/w)

1. Dissolve 3 grams of agar in 150 mL of MilliQ, while stirring and heated to 85°C (oil bath ~ 90°C).
2. Weight and add 3 grams of silica to the same round bottom flask.
3. Maintain at 85°C, stirring for 30 minutes.
4. Cool down to 50°C (keep stirring while cooling) (~1hour)
5. Put a beaker in an ice bath (fast cooling is needed for a homogeneous gel).
6. Cover the gel with parafilm and keep in the fridge.

B: Preparation of smaller gels for liposomes and control solutions

2 % agarose + 2 % silica (w/w)

1. Dissolve 1 gram of agarose in 50 mL MilliQ, while stirring and heated to 85 °C.
2. Weight and add 1 gram of silica.
3. Maintain at 85 °C and keep stirring (~30 minutes).
4. Cool to 50 °C (~ 40 minutes).
5. Cool to 37 °C.
6. Transfer 11 mL of the gel to falcon tube.
7. Put tubes in water bath at 37 °C.
8. After 1 hour, vortex tube and add 1 mL of liposomes.
9. Vortex the tube/mix the liposomes well for homogeneous distribution.
10. Quickly pour the liposomes into a small beaker in an ice bath for fast cooling.
11. Liposomes at this stage have been diluted 12 x.

Appendix V – Additional Results

Deferoxamine Fe(III) Loaded DPPGOG-TSLs

Fe-deferoxamine loaded DPPGOG-TSLs with HBS as intraliposomal buffer

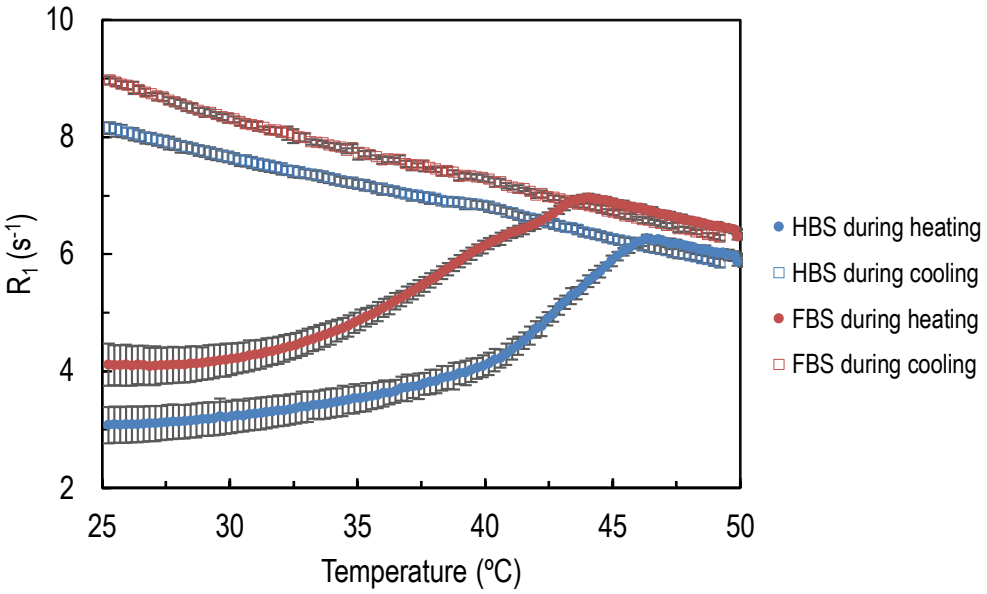

Figure 46. *Inverse T_1-relaxation times of liposomes during a linear temperature increase (0.25 ºC /min) from 23 ºC to 52 ºC, probed at 1.41 T. Shown are DPPGOG-TSLs encapsulating Fe-DFO diluted in HBS (blue) or in FBS (red). Each curve was measured three times.*

In previous work [48] citrate was used as buffer since doxorubicin was being loaded which required an acidic milieu. In this experiment HBS was used instead as the acidic milieu is no longer needed.

The liposomes were leaky at 37 ºC, in HBS (data not shown). Measuring the R_1 at 1.41 T, at 37 ºC for two hours the value was higher than the R_1 expected and seen (before releasing the contrast agent) in the heating cooling curve, Figure 46.

Deferoxamine N-succimidyl Fe(III) Loaded DPPGOG-TSLs

Deferoxamine N-succimidly Fe(III) lloaded DPPGOG-TSLs with Trizma as intraliposomal buffer

Paramagnetic DPPGOG-TSLs were prepared, encapsulating DFO-N-suc-Fe(III) complex as T_1 MRI contrast agent in order to try to improve stability. The DFO-N-suc-Fe(III) complex was passively encapsulated during hydration and subsequent extrusion process. This process yielded DFO-N-suc-Fe(III) filled liposomes with a hydrodynamic radius of around 59.40 nm and a PD.I of 0.086, Figure 47, measured with dynamic light scattering.

Trizma buffer was used since a higher pH is needed to encapsulate DFO-N-suc-Fe(III) complex, since DFO-N-suc-Fe(III) complex is a hydrophilic molecule. The only structural difference between the old compound, Fe-DFO, and DFO-N-suc-Fe(III) complex is that we got rid of the NH_2 group, Figure 14.

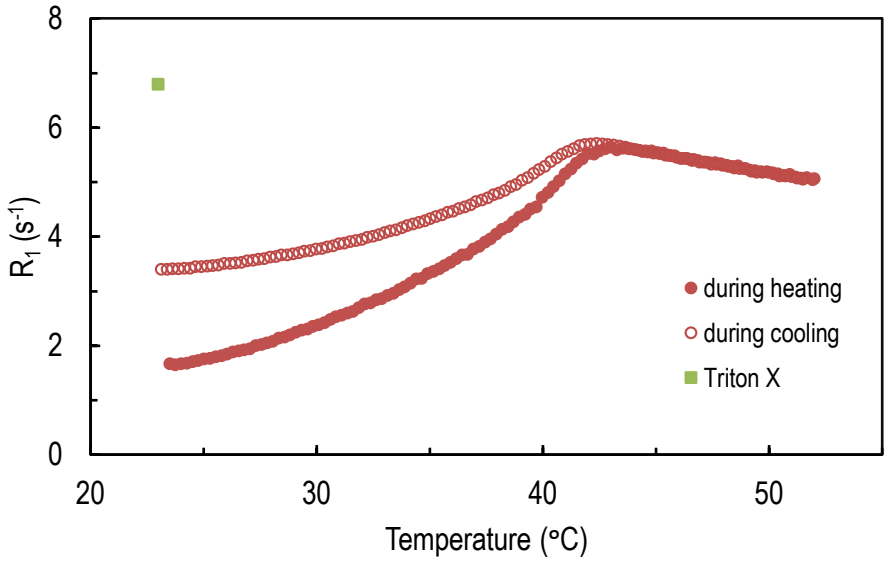

Figure 47. *Inverse T_1-relaxation times of liposomes during a linear temperature increase (0.25 °C/min) from 23 °C to 52 °C and temperature decrease from 52 °C to 23 °C, probed at 1.41 T. Shown are DPPGOG-TSLs encapsulating DFO-N-suc-Fe(III) complex diluted in 90 % FBS.*

There were some problems trying to encapsulate the new DFO derivative and release/stability curves were not acquired. Only 100 mM of DFO-N-suc-Fe(III) complex were encapsulated instead of the expected 240 mM of DFO-N-suc-Fe(III) complex. Only a heating cooling curve was measured which gave the impression of partial release, as it can be seen in Figure 47. The R1 in the end of the cooling was expected to be the same as the R1 after adding 5 µL of Triton X-100.

The pH of the Trizma buffer is temperature dependent which also could be a cause for the unexpected heating cooling curve, suggesting partial release.

Deferoxamine N-succimidly Fe(III) lloaded DPPGOG-TSLs with Gly-Gly as intraliposomal buffer

Next the DPPGOG-TSLs encapsulating DFO-N-suc-Fe(III) complex and using Trizma as a buffer the same experiment was reproduced just changing the Trizma buffer by gly-gly as intraliposomal buffer. Since the pH of the Trizma buffer was temperature-dependent, gly-gly buffer could be a possible alternative to use *in vivo*. This process yielded liposomes with a hydrodynamic radius of around 88.86 nm and a PD.I of 0.0916, measured with dynamic light scattering.

In the end of the washings the supernatant was clear but the liposomes were not as orange as seen and expected in the previous experiments, Figure 48.

Figure 48. *First concentration step just to get rid of unencapsulated iron (left); last washing step, the supernatant looks clear but the liposomes are not orange as expected (right).*

Deferoxamine N-succimidyl Fe(III) Loaded TTSLs

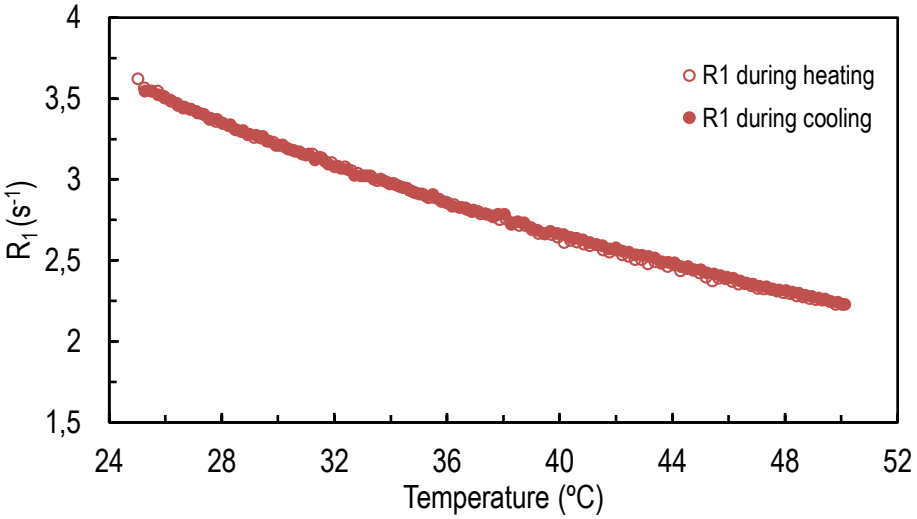

Figure 49. *Longitudinal rate of Deferoxamine-N-succimidyl Fe(III) complex during heating and cooling from 25 ºC to 50 ºC with 0.25 ºC/min.*

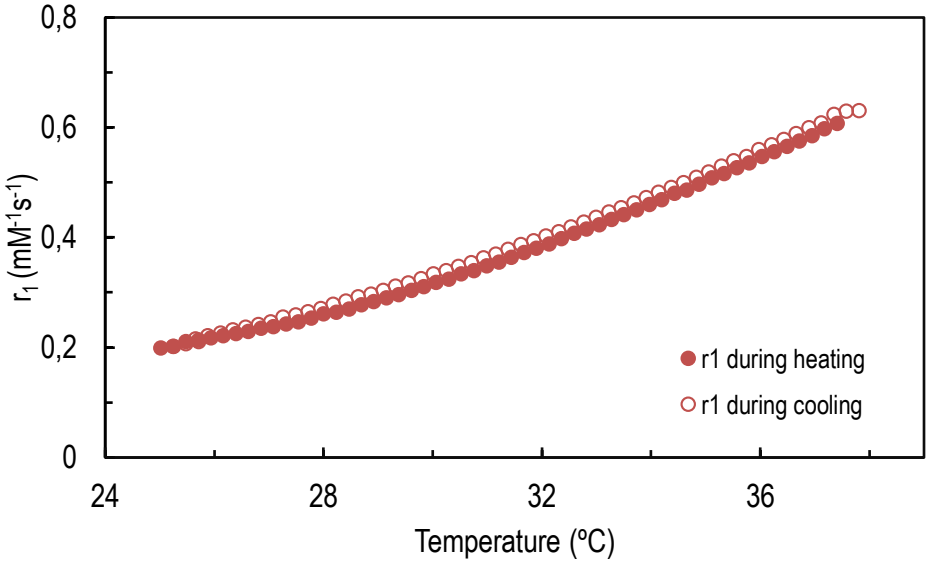

Figure 50. *The longitudinal relaxivity of TTSLs containing DFO-N-suc-Fe(III) complex in HBS during heating from 25 ºC to 38 ºC (0.25 ºC /min) and cooling.*

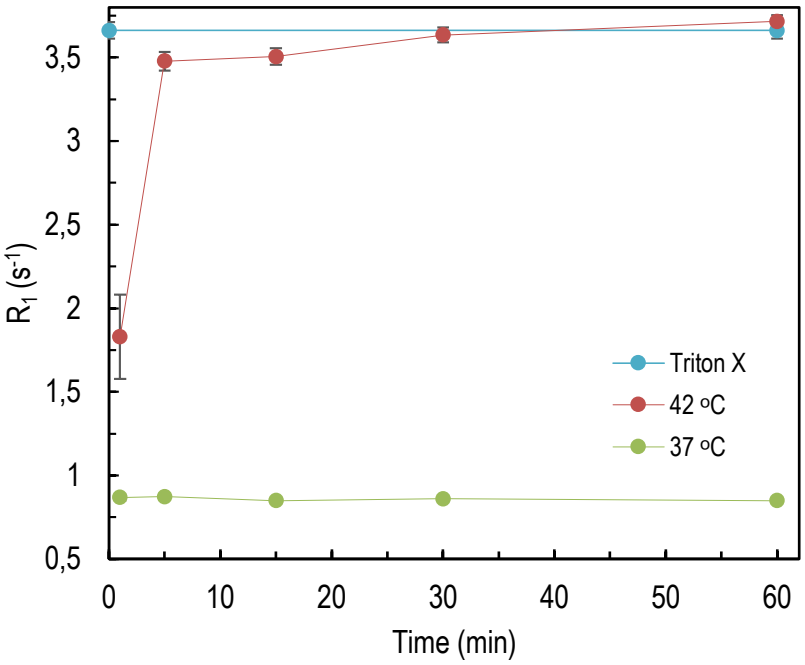

Figure 51. *Release of encapsulated DFO-N-suc-Fe(III) complex from the liposomal system measured at 1.41 T in HBS.*

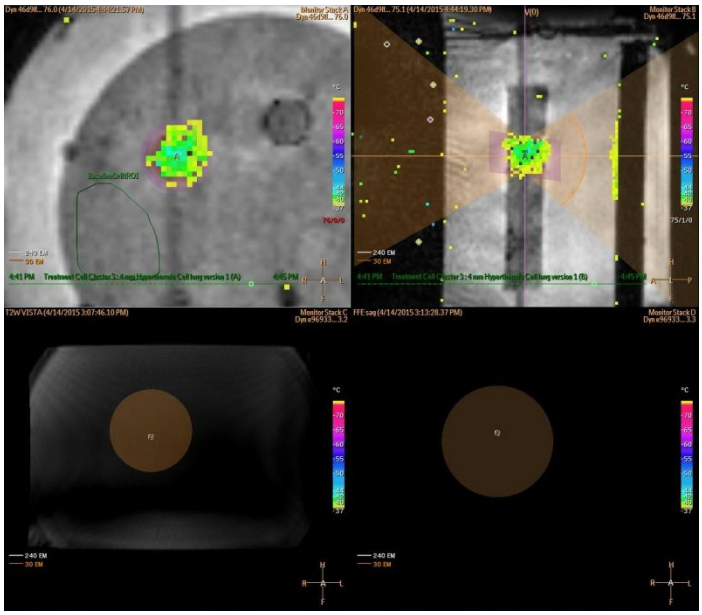

Figure 52. *HIFU mediated release in a gel phantom. Here the upper left agarose spot was exposed to HIFU, while the upper right is serving as a control.*

Cryo-TEM studies of Fe-containing liposomes

Sample: TTSL (lipids: HSPC, DPPC, Cholesterol, DPPE-PEG2000) with iron deferoxamine succinimide.

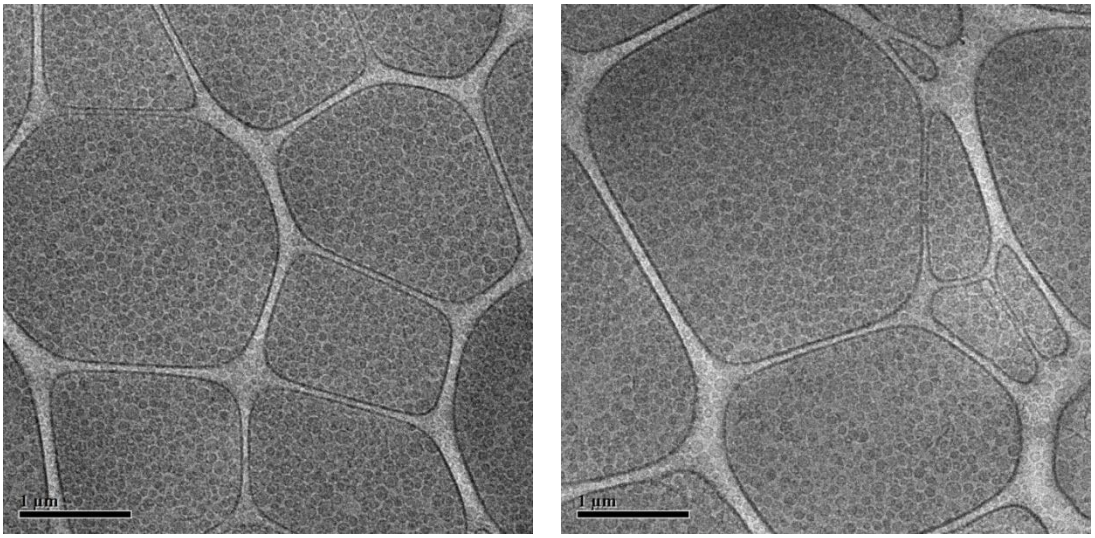

Figure 53. *Overview images showing the typical particles that are present on the TEM sample (magnification: 5,600x).*

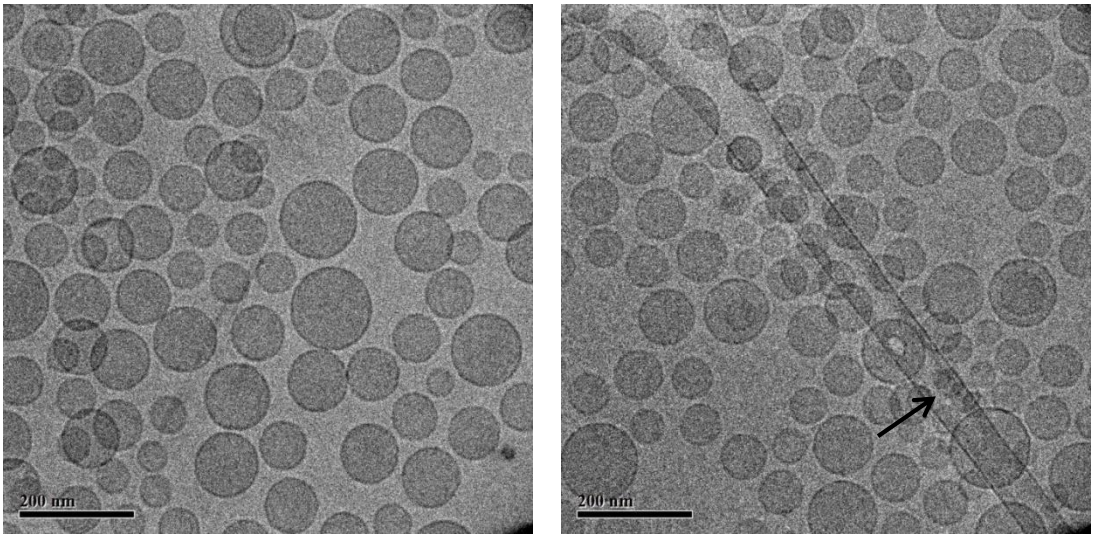

Figure 54. *More detailed images (28,500x).The bright sphere in the right image is most likely a hole in the ice-layer (see black arrow).*

Doxorubicin Loaded TTSLs

The results of the previous set of experiments with deferoxamine N-succimidyl Fe(III) loaded TTSLs were good. Since the idea would be to co-inject both liposomes with the drug and liposomes with the contrast agent the next step would be to investigate the release of doxorubicin from TTSLs since the same formulation of liposomes should be used to the drug and the contras agent, TTSLs.

The slow and incomplete release of doxorubicin from the TTSLs encapsulating only doxorubicin was not expected, Figure 55, as the same TTSL formulation containing both Dox and Gd shows a much faster and complete release [39]. Since the same liposome formulation, was used and only the encapsulated substances differed, only doxorubicin or doxorubicin and gadolinium, one possible explanation can be that the combination of gadolinium and doxorubicin influences the release.

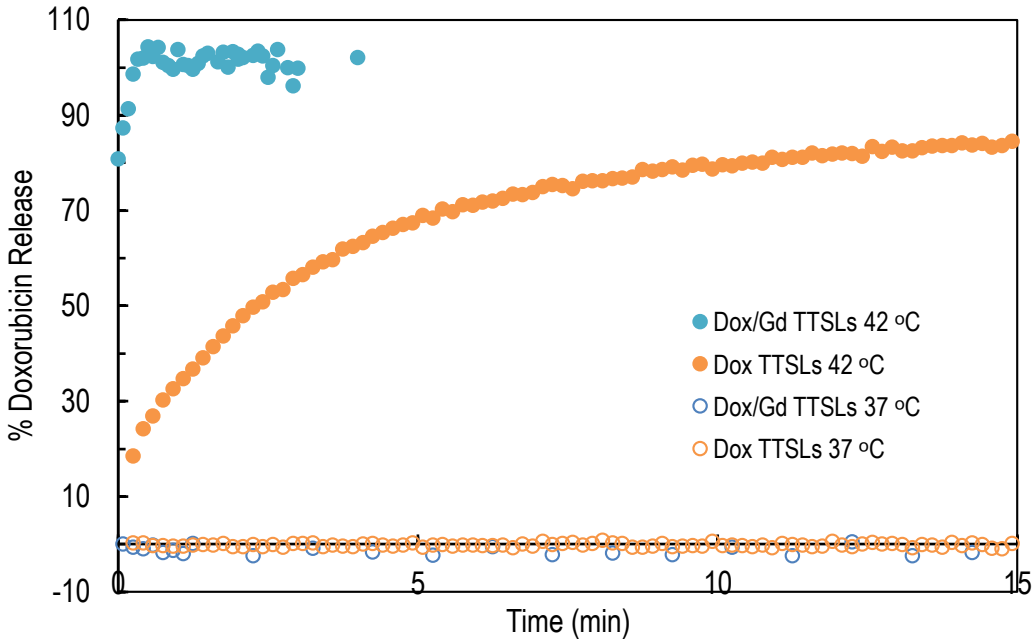

Figure 55. *Release of doxorubicin from TTSLs (encapsulating only doxorubicin) in HBS (HEPES buffered saline) from samples preheated to 37 ºC and 42 ºC (blue) and release of doxorubicin from TTSLs (encapsulating both doxorubicin and gadolinium) in HBS. The percentage of doxorubicin released was calculated from the fluorescence intensities which were measured over time.*

In order to co-release liposomes with doxorubicin and liposomes with DFO-N-suc-Fe(III) complex the release rate of both substances should be similar as was the case for doxorubicin and [Gd(HPDO3A)(H2O)] when encapsulated in the same liposome [39].

Acknowledgements

With only few words I want to enunciate and express my gratitude to everyone who assisted, advised and supported me during this project. Only with the help of others this work was possible.

To begin I would like to thank Holger Grüll, who accepted me in the institute, for the chance to experience this internship abroad, for all the motivation and support.

I would also like to say thank to Esther Kneepkens with whom I spent the most part of the time during my internship and for everything she taught me, for all the patient and know how. When I grow up I want to be like you.

A special thanks to Klaas Nicolay, who after Holger made possible my stay in the Netherlands. Many thanks to Floortje de Groot and to the Biomedical NMR group that made me feel at home in all the coffee and vlai breaks. Next of course, may thanks to the master-room who tried to teach me everything about the Netherlands beginning with the ice skating event. Thanks to Erica Aussem-Custers for all the help in the chemical lab and with my persistent doubts. I would also like to thank SyMO-Chem, Eindhoven, who have contributed to my rewarding work.

Cátia, Marco and Lara, my dutch/portuguese flatmates, my 'family' for helping me with the dutch language, the city and everything I needed. I cannot forget Joana, Ana and my international friends in Eindhoven, who made my days much easier.

Thanks to Professor Nuno Matela who instantly accepted to be my supervisor in Portugal and was always ready to help answering very quickly to my emails.

Many thanks to all my friends and huge family in Portugal, especially to the ones that visited me in Eindhoven and João for the emotional support. Lastly, the biggest thank goes to my parents and brother, for all the financial support and more important for their trust in me, providing me this experience, without them nothing of this would have been possible.